Paleobiology, 41(2), 2015, pp. 280–312
DOI: 10.1017/pab.2014.14

A multivariate approach to infer locomotor modes in Mesozoic mammals

Meng Chen and Gregory P. Wilson

Abstract.—Ecomorphological diversity of Mesozoic mammals was presumably constrained by selective pressures imposed by contemporary vertebrates. In accordance, Mesozoic mammals for a long time had been viewed as generalized, terrestrial, small-bodied forms with limited locomotor specializations. Recent discoveries of Mesozoic mammal skeletons with distinctive postcranial morphologies have challenged this hypothesis. However, ecomorphological analyses of these new postcrania have focused on a single taxon, a limited region of the skeleton, or have been largely qualitative.

For more comprehensive locomotor inference in Mesozoic mammals, we applied multivariate analyses to a morphometric data set of extant small-bodied mammals. We used 30 osteological indices derived from linear measurements of appendicular skeletons of 107 extant taxa that sample 15 orders and eight locomotor modes. Canonical variate analyses show that extant small-bodied mammals of different locomotor modes have detectable and predictable morphologies. The resulting morphospace occupation reveals a morphofunctional continuum that extends from terrestrial to scansorial, arboreal, and gliding modes, reflecting an increasingly slender postcranial skeleton with longer limb output levers adapted for speed and agility, and extends from terrestrial to semiaquatic/semifossorial and fossorial modes, reflecting an increasingly robust postcranial skeleton with shorter limb output levers adapted for powerful, propulsive strokes. We used this morphometric data set to predict locomotor mode in ten Mesozoic mammals within the Docodonta, Multituberculata, Eutriconodonta, "Symmetrodonta," and Eutheria. Our results indicate that these fossil taxa represent five of eight locomotor modes used to classify extant taxa in this study, in some cases confirming and in other cases differing from prior ecomorphological assessments. Together with previous locomotor inferences of 19 additional taxa, these results show that by the Late Jurassic mammals had diversified into all but the saltatorial and active flight locomotor modes, and that this diversification was greatest in the Eutriconodonta and Multituberculata, although sampling of postcranial skeletons remains uneven across taxa and through time.

Meng Chen and Gregory P. Wilson. Department of Biology, University of Washington, Seattle, Washington 98195, U.S.A. E-mail: mengchen@uw.edu; gpwilson@uw.edu

Accepted: 14 October 2014
Published online: 24 February 2015
Supplemental materials deposited at Dryad: doi:10.5061/dryad.870j3

Introduction

During the Mesozoic Era, mammals underwent critical morphological transformations that shaped their evolution and ecology and likely those of modern mammals (e.g., Kielan-Jaworowska et al. 2004). Previous studies of these transformations have mostly focused on the skull and dentition (e.g., tri-ossicular middle ear [Allin and Hopson 1992; Rowe 1996], tribosphenic molar [Luo et al. 2001a,b], and encephalization [Jerison 1973; Rowe et al. 2011]). Inferences about the evolution of locomotor complexes, locomotor diversity, and the role of locomotion and substrate use in resource partitioning among Mesozoic mammals have historically been hampered by a fossil record of mostly dental specimens, some cranial material, and very few postcranial skeletons (e.g., Kielan-Jaworowska et al. 2004). However, in the last three decades, a large number of relatively complete skeletons of early mammals have been reported, most notably from the Upper Jurassic and Cretaceous of Asia (e.g., Kielan-Jaworowska and Gambaryan 1994; Hu et al. 1997; Ji et al. 1999, 2006; Horovitz 2003; Luo et al. 2003, 2007; Meng et al. 2006; Hurum and Kielan-Jaworowska 2008; Yuan et al. 2013; Zhou et al. 2013).

Based on anatomical and functional insights from these newly recovered, more complete fossils, Luo (2007) challenged the traditional notion that all Mesozoic mammals were small-bodied, ecologically generalized, terrestrial forms. Instead, he proposed that Mesozoic mammals occupied a broad range of ecological

© 2015 The Paleontological Society. All rights reserved. 0094-8373/15

categories, approaching the diversity found among modern communities of small-bodied mammals. Here, we aim to (i) develop a robust quantitative approach to infer locomotion and substrate use in Mesozoic mammals and (ii) apply it to select taxa to assess the breadth of locomotor specializations among Mesozoic mammals.

Background

Today's mammals include more than 5000 species in 29 orders (Wilson and Reeder 2005) that range from the tiny (~2 g), aerial bumblebee bat to the titanic ($\sim 100 \times 10^3$ kg), fully aquatic blue whale. They inhabit a broad range of habitats from the bottom of the oceans to inhospitable deserts and mountain snow lines (Wilson and Reeder 2005). This diversity is in part due to morphological evolution of the postcranial skeleton. Not only does the rigid postcranial skeleton structurally support an animal's body mass and outline its shape, but it also acts through coordinated neuromuscular pathways to move the animal through its environment (e.g., Grillner and Wallén 1985; Kardong 2009).

Whereas numerous methods have been developed to infer feeding ecology in fossil mammals (e.g., microwear, dental complexity, geometric morphometrics [Ungar and Williamson 2000; Wilson et al. 2012; Evans 2013; Wilson 2013]), few quantitative approaches have been developed to infer mammalian locomotion and substrate use and fewer have been applied to Mesozoic mammals. Those that have been developed use the relationship between postcranial morphology and locomotion/substrate use in living forms as an analogue (e.g., Van Valkenburgh 1987; Stein 1988; Sargis 2001a, 2002a,b; Gingerich 2003; Elissamburu and Vizcaíno 2004; O'Keefe and Carrano 2005; Kirk et al. 2008; Polly 2008, 2011; Samuels and Van Valkenburgh 2008; Fröbisch and Reisz 2009; Samuels et al. 2013). Unfortunately, most of these studies have focused on (i) no more than a few skeletal elements (e.g., distal phalanges [MacLeod and Rose 1991], autopodial skeleton [Weisbecker and Schmid 2007], third digit ray [Kirk et al. 2008]); (ii) a narrow phylogenetic scope (e.g., Tupaiidae [Sargis 2001a, 2002a,b], Diprotodontia [Weisbecker and Warton 2006], Rodentia [Samuels and Van Valkenburgh 2008]); (iii) single or few locomotor modes (e.g., fossorial mode [Hopkins and Davis 2009]; and/or (iv) mostly large-bodied taxa (>5 kg; e.g., Van Valkenburgh 1987; Gingerich 2003; Samuels et al. 2013). None have focused on a phylogenetically broad sample of small-bodied mammals (≤5 kg) that could be used as an analogue for Mesozoic mammals.

Here, we describe and validate a new method to quantitatively infer locomotor mode in small-bodied fossil mammals. This method uses functionally relevant, linear measurements that are broadly distributed across the appendicular skeleton. Relative to other measurement schemes that focus on only one or a few postcranial elements, our more extensive scheme (i) accounts for conflicting locomotor signatures from different parts of the skeleton, and (ii) enables discrimination among locomotor modes that share similar values for one or a few osteological indices. Moreover, we sampled nearly half of all mammalian orders and eight locomotor modes. The inclusion of a broad diversity of taxa in each mode minimizes the phylogenetic overprint that can confound ecomorphological associations. From this data set, we analyzed linear measurement ratios, using canonical variate analysis. Our results show that the different locomotor modes occupy distinct regions of the morphospace, indicating that postcranial morphology can be used to predict locomotor mode in small-bodied mammals. Thus, we used this approach and data set to infer locomotor mode in a taxonomically and morphologically diverse sample of Mesozoic mammals.

Materials and Methods

Taxa

Our extant mammalian data set includes measurements from 107 extant species from 15 orders: Afrosoricida, Carnivora, Cingulata, Dasyuromorphia, Didelphimorphia, Diprotodontia, Erinaceomorpha, Lagomorpha, Macroscelidea, Monotremata, Peramelemorphia, Primates, Rodentia, Scandentia, and Soricomorpha (Fig. 1, Supplementary Table 1). For each species, we sampled one adult individual. Additional sampling and strict sampling of

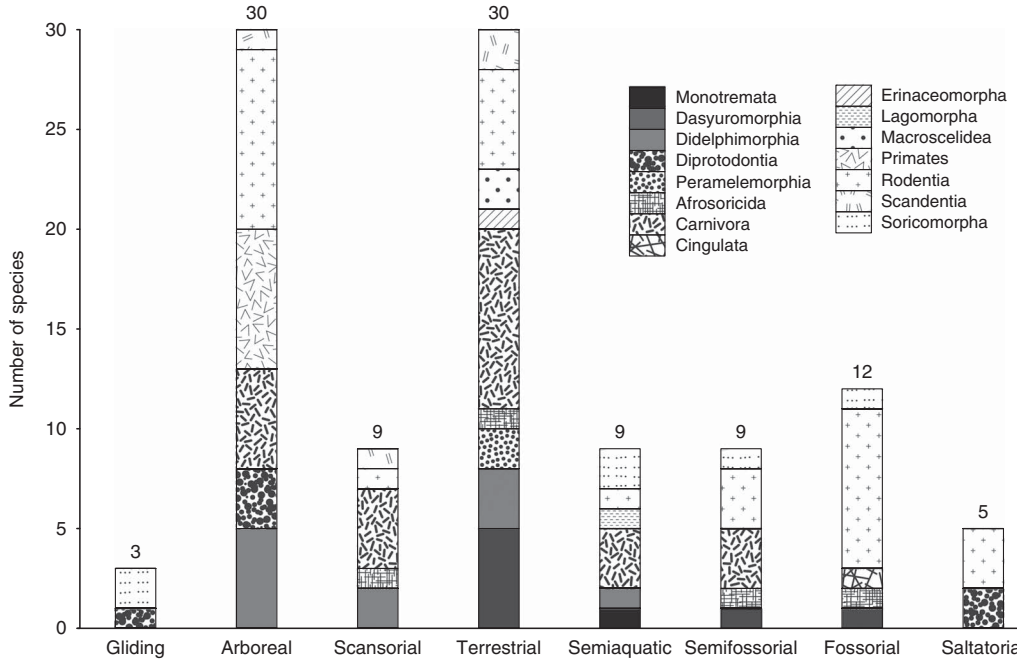

FIGURE 1. Taxonomic sampling of extant small-bodied mammals in each locomotor mode in our data set. Numbers indicate the total number of species of each locomotor order that are included.

only field-collected specimens unfortunately were hampered by variability in the degree of completeness and quality of preservation among museum specimens of the same species. However, whenever possible we examined additional specimens of the same species to confirm that the postcranial morphology of our measured specimen was representative for that species. Skeletons were identified as those of adults based on dental eruption pattern, epiphyseal fusion, or both. Although the degree of sexual dimorphism among small-bodied mammals is usually minor, we attempted to control for it by measuring specimens of male individuals whenever possible. We selected mostly small-bodied species ($\leq$5 kg, following Bourlière 1975; Stoddart 1979; Degen 1997; Merritt 2010) to reflect the typical body size of most Mesozoic mammals (e.g., Lillegraven et al. 1979; Kielan-Jaworowska et al. 2004). A few select species have body masses up to 16 kg (e.g., *Vulpes vulpes*), which represent the estimated upper limit for Mesozoic mammals (e.g., *Repenomamus giganticus* [Hu 2006]). Species were also selected to cover a broad range of locomotor strategies. We excluded flying mammals (i.e., bats) from our extant mammalian data set because flying mammals have not yet been reported from the Mesozoic. Owing to their high taxonomic richness and abundance, rodents and carnivorans are particularly well represented in museum collections and, in turn, our data set (Fig. 1). See Supplementary Table 1 for details.

We also measured postcranial skeletons of ten fossil taxa that broadly sample the phylogenetic diversity and evolutionary history of Mesozoic mammals. The sample consists of four eutriconodontans, one multituberculate, two symmetrodontans, and one eutherian, all from northeastern Asia; one docodontan from Western Europe (Portugal); and the enigmatic *Fruitafossor* from North America. Most included specimens are published: the Late Jurassic *Fruitafossor windscheffeli* (Luo and Wible 2005); the Late Jurassic docodontan *Haldanodon exspectatus* (Martin 2005, 2013); the Late Jurassic multituberculate *Rugosodon eurasiaticus* (Yuan et al. 2013); the Early Cretaceous eutriconodontans *Jeholodens jenkinsi* (Ji et al. 1999), *Repenomamus robustus* (Hu et al. 2005; Hu 2006), and *Yanoconodon allini* (Luo et al. 2007); the Early Cretaceous symmetrodontan *Akidolestes cifellii* (Li and Luo 2006; Chen and Luo 2013); and the Early Cretaceous eutherian

TABLE 1. Inferred locomotor modes of Mesozoic mammals. Abbreviations: ELM, eight-locomotor-mode analysis; FLM, five-locomotor-mode analysis; NI, number of osteological indices; NM, number of measurements; *p*, posterior probability.

Taxon	Order	Specimen no.	NM	NI	Inferred locomotor mode	
					ELM (*p*)	FLM (*p*)
Haldanodon exspectatus	Docodonta	Gui Mam 30/79	21	21	A/Sf/T (56.6%/41.6%/1.8%)	Sf (100%)
Fruitafossor windscheffeli	N/A	LACM 150948	25	23	F (100%)	N/A
Repenomamus robustus	Eutriconodonta	IVVP V12728	28	22	Sf (100%)	Sf (100%)
Liaoconodon sp.	Eutriconodonta	BMNH PM001139	35	24	Sa (100%)	Sa (99.7%)
Yanoconodon allini	Eutriconodonta	NJU-P06001	30	27	Sa (99.7%)	Sa (99.9%)
Jeholodens jenkinsi	Eutriconodonta	GMV 2139	40	25	A (98.8%)	A/T (73.9%/21.2%)
Rugosodon eurasiaticus	Multituberculata	BMNH PM001142	35	24	A (98.8%)	Sc (94.8%)
Akidolestes cifelli	"Symmetrodonta"	NIGPAS 139381	35	27	Sf (99.3%)	Sf (99.8%)
Zhangheotherium sp.	"Symmetrodonta"	DMNH 2874	27	16	Sf/Sc/A/T (32.6%/26.2%/20.0%/11.6%)	Sc/T (71.3%/12.2%)
Eomaia scansoria	Eutheria	CAGS01-IG1	31	24	A/Sc/T (68.6%/16.5%/11.3%)	A (93.2%)

See *Methods and Materials* for abbreviations of institutions and locomotor modes.

Eomaia scansoria (Ji et al. 2002). We also included two unpublished specimens from the Early Cretaceous: the eutriconodontan *Liaoconodon* sp. indet. and symmetrodontan *Zhangheotherium* sp. indet. Among the ten Mesozoic taxa, eight have previously been assigned to locomotor modes based on a more traditional comparative anatomy approach (Hu et al. 1997, 1998; Ji et al. 1999, 2002; Luo and Wible 2005; Martin 2005; Hu 2006; Li and Luo 2006; Luo et al. 2007; Chen and Luo 2013; Yuan et al. 2013) (Table 1). Because the degree of completeness varies among these specimens, each taxon has a unique set of available postcranial measurements. Thus, when inferring locomotor mode in these fossil taxa, we could not use a universal morphometric data set of extant small-bodied mammals, but instead individually pruned the modern data set to reflect the measurements available for each fossil specimen.

Extant specimens were accessed in the mammal collections of the American Museum of Natural History (AMNH), New York, New York; the Field Museum of Natural History (FMNH), Chicago, Illinois; the Smithsonian Institution National Museum of Natural History (NMNH), Washington, D.C.; and the University of Washington's Burke Museum of Natural History and Culture (UWBM), Seattle, Washington. Eight of the fossil specimens are housed in Chinese institutions: the Beijing Museum of Natural History (BMNH), Beijing; the Chinese Academy of Geological Sciences, Institute of Geology (CAG-IG), Beijing; the Institute of Vertebrate Paleontology and Paleoanthropology, Chinese Academy of Science (IVPP), Beijing; the National Geological Museum of China (GMV), Beijing; the Dalian Museum of Natural History (DMNH), Dalian; the Nanjing Institute of Geology and Paleontology, Chinese Academy of Science (NIGPAS), Nanjing; the Nanjing University (NJU), Nanjing. The other two fossil specimens are housed in the Museu Geológico (Gui Mam), Lisbon, Portugal, and the Los Angeles County Museum (LACM), Los Angeles, California, U.S.A.

Locomotor Modes

We used natural history compendia and the primary literature (e.g., Howell 1930; Nowak 1999, 2005; Wilson and Reeder 2005;

TABLE 2. Definitions of locomotor modes of small-bodied mammals that were used in this study (modified from Hildebrand and Goslow 1998; Polly 2007; Samuels and Van Valkenburgh 2008; Samuels et al. 2012).

Locomotor mode	Descriptive definition
Gliding	Bridge gaps between trees by gliding usually with patagium
Arboreal	Spend most of the time in trees foraging, traveling, resting, but occasionally travel on the ground
Scansorial	Capable of climbing for escape, eating, or leisure, and probably spend a considerable time both in the trees and on the ground
Terrestrial	Spend most of time on the ground, but able to swim, climb, and burrow occasionally, but not specialized for those
Semiaquatic	Capable of swimming for dispersal, escape, or foraging as well as on the ground
Semifossorial	Regularly dig for food or to build burrows for shelter, but do not exclusively live underground
Fossorial	Efficiently dig burrows for shelter or foraging underground exclusively
Saltatorial	Capable of jumping using both hind limbs simultaneously for high-speed transportation over long distance

Samuels and Van Valkenburgh 2008; Samuels et al. 2013) (Supplementary Table 1) to assign each extant species to one of eight locomotor modes: gliding (G), arboreal (A), scansorial (Sc), terrestrial (T), semifossorial (Sf), fossorial (F), semiaquatic (Sa), or saltatorial (S) (Table 2). These modes are commonly used in those natural history compendia and the primary literature. Owing to limited availability, most small-bodied primates included in this study are callitrichines that have a specialized arboreal locomotion relative to other primates. Because of the adaptations involved in gliding from tree to tree, we treated gliding mammals as a separate locomotor mode, although they commonly have an arboreal lifestyle.

Postcranial Measurements and Indices

We took 45 linear measurements of the appendicular postcranial skeleton (Fig. 2, Supplementary Table 2). Some of these measurements have been included in other studies, where they were shown to be functionally relevant or important for discriminating among locomotor strategies (Supplementary Table 2) (e.g., Van Valkenburgh 1987; Beard 1993; Sargis 2001a, 2002a,b; Samuels and Van Valkenburgh 2008; Samuels et al. 2013). We primarily used Mitutoyo Digimatic Digital Calipers (±0.05 mm accuracy) to collect these measurements. For very small elements, we captured high-resolution images with a digital camera (Nikon D80) and then obtained measurements using NIH ImageJ 64 software for Mac (±0.01 mm accuracy). This method was also used for measuring the postcranial elements of the fossil mammals on high-resolution photographs of *Akidolestes cifellii, Jeholodens jenkinsi, Liaoconodon* sp., *Repenomamus robustus, Rugosodon eurasiaticus, Yanoconodon allini*, and *Zhangheotherium* sp., and published figures of *Eomaia scansoria* (Ji et al. 2002), *Fruitafossor windscheffeli* (Luo and Wible 2005), and *Haldanodon exspectatus* (Martin 2005).

To reduce the size correlation within the data matrix, we converted the linear measurements to ratios of bony elements or bony features (osteological indices). Some of the osteological indices reflect functional morphology (Samuels and Van Valkenburgh 2008). For example, the Olecranon Process Length Index (OPLI) captures the relative length of the input-lever of the forearm; an increase in OPLI would imply a greater capacity to generate output forces by the triceps brachii, which is a common adaptation to semiaquatic, semifossorial, and fossorial modes. Sokal and Rohlf (2012) cautioned that statistical analyses of ratios might potentially violate the assumptions of normality and homoscedasticity for parametric tests as well as some other problems noted by Emerson (1985). However, Carrano (1999) argued that without a uniform denominator, spurious intercorrelation might not cause a statistical problem. Arcsine transformation has been forwarded as a solution to this potential statistical violation (Sokal and Rohlf 2012), but our data set includes ratios greater than 1.0 that are not amenable to arcsine transformation. Previous studies have produced robust ecomorphological inferences of fossil taxa by using raw osteological indices (Van Valkenburgh 1987; Van Valkenburgh

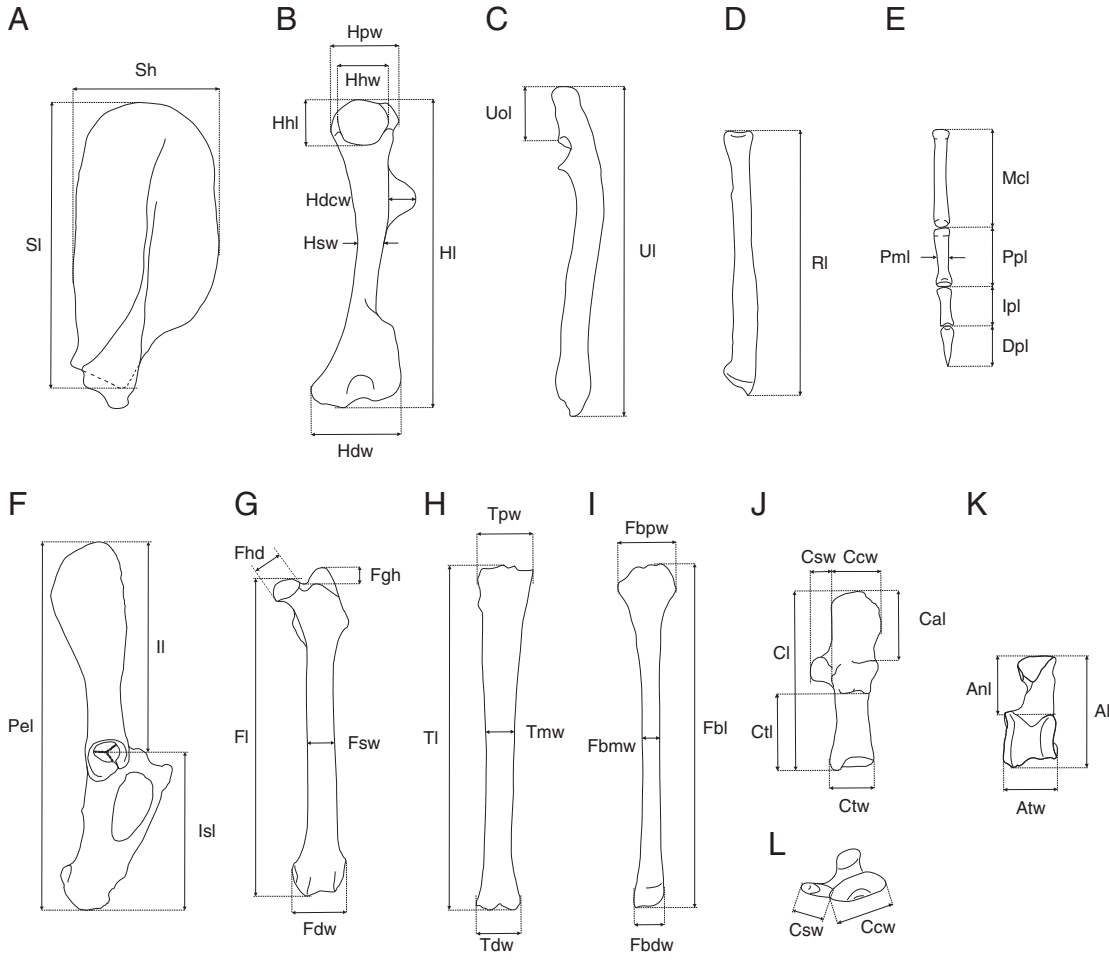

FIGURE 2. Schematic of the linear measurements obtained from the appendicular skeleton of extant and extinct small-bodied mammals. A, Scapula (lateral view). B, Humerus (posterior view). C, Ulna (lateral view). D, Radius (posterior view). E, Ray III of manus (dorsal view). F, Pelvis (lateral view). G, Femur (anterior view). H, Tibia (anterior view). I, Fibula (anterior or lateral view). J, Calcaneus (dorsal view). K, Astragalus (dorsal view). L, Calcaneus (anterior view). See Supplementary Table 2 for full descriptions of the postcranial skeletal measurements. A, C, D, E, G, H, I, and L are from the left side, and B, F, J, and K are from the right side.

and Koepfli 1993; Elissamburu and Vizcaíno 2004) or transformed osteological indices (Samuels and Van Valkenburgh 2008; Bover et al. 2010; Samuels et al. 2013) in their multivariate analyses. On this basis, we converted the 45 linear measurements from our modern data set to 56 osteological indices (Table 3), and then determined how well each raw osteological index discriminated among locomotor modes (see *Statistical Analyses*, below). For ease of communication and interpretation, we grouped the osteological indices into three major types: (1) robustness indices, which describe the robustness of postcranial elements; (2) morphofunctional indices, which reflect functional aspects of morphology, such as length of an input lever, and (3) proportional indices, which describe the shape or relative size of a postcranial element (Bover et al. 2010).

Statistical Analyses

To test whether there were significant differences across the eight locomotor modes in each osteological index, we carried out 56 univariate analyses of variance (ANOVA). Then, we used the osteological indices that were significantly different across eight locomotor modes ($p < 0.001$) in the canonical variate analysis

(CVA) to determine the linear combination of variables that maximize segregation among our eight locomotor modes. To enhance segregation among some tightly clustered locomotor modes, we also successively pruned the data sets down to five and three locomotor modes for two additional CVAs. We refer to these analyses as the eight-, five-, and three-locomotor-mode analyses, respectively. The same prior probability was given to each locomotor mode in the CVA to correct the uneven sampling of the eight locomotor modes. Together, the CVAs identify morphological signatures (via osteological indices) of the appendicular skeleton for each locomotor mode in our extant mammalian data set. We used the first three canonical functions (CFs) in the eight-locomotor-mode analysis to calculate the morphological variance, the mean of the squared-distance from each data point to the centroid, within each locomotor mode.

We then used this training set as a basis to predict locomotor habit in ten Mesozoic mammal species for which we obtained the same linear measurements. We initially conducted the multivariate analyses for each Mesozoic species, using the modern data set comprising all eight locomotor modes. In that analysis, more specialized locomotor modes (gliding, saltatorial, or fossorial) are well segregated, but the remaining modes (arboreal, scansorial, terrestrial, semiaquatic, and semifossorial) cluster together. Because *Fruitafossor* is the only Mesozoic taxon likely to have had an extremely specialized locomotor mode (fossorial [Luo and Wible 2005]), we conducted secondary analyses on the other nine fossil mammals by removing the specialized modes from the data set (five-locomotor-mode analysis). We chose not to perform a three-locomotor-mode analysis because it would preemptively narrow the possible locomotor inferences. The ANOVA and CVA were carried out using RStudio 0.98.501 (R core v3.1.0 64-bit). For the ANOVA, we used built-in functions in R, and for the CVA, we used R package MASS 7.3-31 (Venables and Ripley 2002).

To visualize the locomotor morphospace occupied by the extant small-bodied mammals in our data set, we plotted the CF1, CF2, and CF3 scores in bivariate plots. In all of our analyses, the first three CFs account for more than 85% of the variance (Supplementary Tables 3, 6, and 8 show the variance explained by each CF in each analysis).

Results

Morphological Variation among Locomotor Modes

ANOVA results indicate that 30 of the 56 osteological indices are significantly different across eight locomotor modes ($p < 0.001$) (Table 4). We suggest that these indices capture the morphological variation that is important for characterizing the eight locomotor modes.

Among our locomotor modes, gliding, arboreal, fossorial, and saltatorial mammals exhibit more-specialized morphological signatures (Table 5, Fig. 3A,B). Given that certain arboreal supports cannot withstand great amounts of weight, many gliding and arboreal mammals have minimized their body mass and have enhanced their locomotor dexterity and precision for movement in the trees in order to reduce the risk of falling from trees. Thus, they have more-gracile bony elements than taxa that exhibit different locomotor modes. In turn, most of the morphological signatures of the arboreal and gliding modes reflect low robustness indices, including (i) a slender humerus with small and round humeral head (HRI, HHRI, and HHw:Hpw; see Table 3 for definition), (ii) a weakly developed humeral deltopectoral crest (DI), (iii) a small olecranon process of the ulna (OPLI), (iv) a small palm with slender, elongate phalanges (PRTI and PI), (v) an elongate ilium (IRI), (vi) a gracile femur and tibia (FRI and TRI), (vii) a small greater trochanter (GI), and (viii) an elongated calcaneal body and a shortened calcaneal tuber (CBRI and CTRI). Scansorial taxa, which are capable of climbing but do not inhabit trees, are intermediate in form between arboreal and terrestrial taxa and possess a relatively long forelimb (IM). Terrestrial mammals have a moderately built (i) deltopectoral crest of the humerus (DI), (ii) olecranon process of the ulna (OPLI), and (iii) greater trochanter of the femur (GI), as well as a relatively short (iv) ulna (Ul:Hl; see Table 3 for definition) and (v) phalanges (PI and MRTI).

TABLE 3. List of the osteological indices that were used in this study and derived from linear measurements of the appendicular skeleton of small-bodied mammals. Codes for the types of osteological indices: 1, robustness index; 2, morphofunctional index; 3, proportional index.

No.	Osteological index	Abbr.	Equation	Description	Selected references for example	Index type
1	Scapular shape index	SI	Sh:Sl	Scapular height divided by scapular length	Sargis 2002a	2
2			Sl:Hl	Scapular length divided by humeral length		3
3	Humerus robustness index	HRI	Hsw:Hl	Humeral mid-shaft transverse diameter divided by humeral length	Elissamburu and Vizcaíno 2004; Samuels and Van Valkenburgh 2008; Bover et al. 2010; Samuels et al. 2013	1
4	Humeral proximal end index	HPI	Hpw:Hl	Humeral proximal end width divided by humeral length		1
5	Humeral epicondylar index	HEB	Hdw:Hl	Humeral epicondylar width divided by humeral length	Elissamburu and Vizcaíno 2004; Samuels and Van Valkenburgh 2008; Bover et al. 2010; Samuels et al. 2013	1
6			Hsw:Hpw	Transverse diameter of humerus divided by humeral proximal end width		3
7	Humeral head robustness index	HHRI	HHl:Hl	Humeral head length divided by humeral length		1
8	Humeral head shape index	HHSI	HHw:HHl	Humeral head width divided by humeral head length	Sargis 2002a	2
9			HHw:Hpw	Humeral head width divided by humeral proximal end width		3
10			Hpw:Hdw	Humeral proximal end width divided by humeral distal width		3
11			HHw:Hdw	Humeral head width divided by humeral distal end width		3
12			Hsw:Hdw	Transverse diameter of humerus divided by humeral distal end width		3
13			Hdw:Sh	Humeral epicondylar width divided by scapular length		3
14			Hdcw:Hpw	Deltopectoral crest width divided by humeral proximal end		3
15	Deltopectoral crest index	DI	Hdcw:Hsw	Deltopectoral crest width divided by the mid-shaft width of humerus		1
16			Hdcw:Hdw	Deltopectoral crest width divided by humeral distal end		3
17			Ul:Hl	Ulnar length divided by humeral length		3
18	Olecranon Process Length Index	OPLI	Uol:Ul	Olecranon process length divided by ulna length	Sargis 2002a	2
19			Uol:Hl	Olecranon process length divided by humeral length		2
20	Brachial Index	BI	Rl:Hl	Radial length divided by humeral length	Sargis 2002a; Samuels and Van Valkenburgh 2008; Bover et al. 2010; Samuels et al. 2013	3

TABLE 3. Continued

No.	Osteological index	Abbr.	Equation	Description	Selected references for example	Index type
21			Rl:Ul	Radial length divided by ulnar length		3
22			Uol:Rl	Olecranon process length divided by radial length		2
23	Palm robustness index	PRTI	Mcl:(Hl + Rl)	Metacarpal length divided by lengths of humerus and radius		2
24	Metacarpal robustness index	MRI	Mcw:Mcl	Transverse diameter metacarpal bone of digit ray III divided by its length		1
25	Proximal phalangeal robustness index	PPRI	Ppw:Ppl	Transverse diameter of proximal phalanx of digit ray III divided by its length		1
26	Intermediate phalangeal robustness index	IPRI	Ipw:Ipl	Transverse diameter of intermediate phalanx of digit ray III divided by its length		1
27	Distal phalangeal robustness index	DPRI	Dpw:Dpl	Transverse diameter of distal phalanx of digit ray III divided by its length		1
28			Dpl:Mcl	Distal phalanx length of digit ray III divided by humeral length		3
29	Phalangeal index	PI	(Ppl + Ipl): Mcl	Lengths of proximal and intermediate phalanges of digit ray III divided by metacarpal length	Beard 1993; Lemelin 1999; Argot 2001; Bloch and Boyer 2002; Ji et al. 2002; Luo et al. 2003; Chen and Luo 2008; Kirk et al. 2008; Chen and Luo 2013	2
30	Phalangeal robustness index	PRI	(Ppl + Ipl + Dpl):Mcl	Lengths of all phalanges divided of digit ray III by metacarpal length		1
31	Manual robustness index	MRTI	(Mcl + Ppl + Ipl + Dpl): (Hl + Rl)	Manual length divided by lengths of humerus and radius		1
32	Ilium robustness index	IRI	Il:Pel	Ilium length divided by entire pelvic length	Sargis 2002b	1
33			Il:Isl	Ilium length divided by ischium length		3
34	Gluteal Index	GI	FGh:Fl	Proximal extension of greater trochanter divided by femoral length	Sargis 2002b; Samuels and Van Valkenburgh 2008; Bover et al. 2010; Samuels et al. 2013	2
35	Femoral robustness index	FRI	Fsw:Fl	Transverse diameter divided by femur length	Elissamburu and Vizcaíno 2004; Samuels and Van Valkenburgh 2008; Bover et al. 2010; Samuels et al. 2013	1
36	Femoral head robustness index	FHRI	Fhd:Fsw	Femoral head diameter divided by femoral mid-shaft width		1
37			Fsw:Fdw	Transverse diameter of femur divided by the femoral distal end width		3
38	Crural Index	CI	Tl:Fl	Tibial length divided by fibular length	Sargis 2002b; Samuels and Van Valkenburgh 2008; Bover et al. 2010; Samuels et al. 2013	3
39	Intermembral index	IM	(Hl + Rl): (Tl + Fl)	Lengths of the humerus and radius divided by lengths of the femur and tibia.	Sargis 2002a; Samuels and Van Valkenburgh 2008; Bover et al. 2010; Samuels et al. 2013	3

TABLE 3. Continued

No.	Osteological index	Abbr.	Equation	Description	Selected references for example	Index type
40			Tmw:Tpw	Transverse diameter of tibia divided by tibial proximal end width		3
41			Tdw:Tpw	Tibial distal end width divided by tibial proximal end width		3
42	Tibial robustness index	TRI	Tmw:Tl	Transverse diameter of tibia divided by tibial length	Elissamburu and Vizcaíno 2004; Samuels and Van Valkenburgh 2008; Bover et al. 2010; Samuels et al. 2013	1
43	Fibular robustness index	FBRI	Fbsw:Fbl	Transverse diameter of fibula divided by fibular length		3
44			Fbsw:Fbpw	Transverse diameter of fibula divided by fibular proximal end width		3
45			Fbdw:Fbpw	Fibular distal end width divided by fibular proximal end width		1
46	Fibular proximal end robustness index	FPRI	Fbpw:Fbl	Robustness of the proximal end of fibula		1
47	Fibular distal end robustness index	FDRI	Fbdw:Fbl	Robustness of the distal end of fibula		1
48	Astragalar neck robustness index	ANRI	Anl:Al	Astragalar neck length divided by astragalar length		1
49	Astragalar trochlea robustness index	ATRI	Atw:Al	Astragalar trochlea width divided by astragalar length		1
50	Calcaneal body robustness index	CBRI	Cal:Cl	Calcaneal body length divided by calcaneal length		1
51	Calcaneal tuber robustness index	CTRI	Ctl:Cl	Calcaneal tuber length divided by calcaneal length		3
52			Cal:Ctl	Calcaneal body length divided by calcaneal tuber length	Bassarova et al. 2009	3
53	Sustentacular robustness index	SRI	Csw:Ccw	Sustentacular process width divided by calcaneal cuboid facet width		1
54	Cuboid facet robustness index	CFRI	Ccw:Cl	Cuboid facet width divided by calcaneal length	Bassarova et al. 2009	1
55			Ctw:Ccw	Calcaneal tuber facet width divided by cuboid facet width		3
56	Tuber facet robustness index	TFRI	Ctw:Cl	Tuber facet width divided by calcaneal length		1

TABLE 4. Means, standard deviations, and results of the univariate ANOVA tests of each osteological index for each locomotor mode. Abbreviations: A, arboreal; F, fossorial; G, gliding; S, saltatorial; Sc, scansorial; Sa, semiaquatic; Sd, standard deviation; Sf, semifossorial; T, terrestrial. Shaded osteological indices were used in canonical variate analyses.

	Mean of each locomotor mode										Multivariate ANOVA Test			
Index No.	G	A	Sc	T	Sa	Sf	F	S	Total Mean	Sd	Sum Square	Mean Square	*F*-value	Pr (>F)
1	0.490	0.580	0.549	0.544	0.558	0.546	0.576	0.512	0.556	0.101	0.05005	0.00715	0.693	0.6778
2	0.590	0.675	0.731	0.759	0.854	0.811	0.948	1.024	0.774	0.164	1.1629	0.166136	9.8412	2.90E-09***
3	0.067	0.083	0.080	0.078	0.098	0.099	0.132	0.090	0.089	0.032	0.03048	0.0043543	5.3921	2.94E-05***
4	0.163	0.182	0.198	0.205	0.260	0.237	0.318	0.246	0.219	0.069	0.19802	0.028289	8.9938	1.51E-08***
5	0.210	0.248	0.227	0.237	0.332	0.303	0.404	0.308	0.274	0.110	0.3419	0.048843	5.1845	4.67E-05***
6	0.413	0.458	0.413	0.381	0.378	0.416	0.403	0.358	0.410	0.060	0.11757	0.0167953	6.4443	2.94E-06***
7	0.123	0.130	0.130	0.135	0.151	0.157	0.188	0.160	0.143	0.029	0.037058	0.0052941	9.8473	2.86E-09***
8	0.990	1.068	1.170	1.114	1.179	1.049	0.880	1.080	1.074	0.210	0.709	0.101287	2.532	0.01938*
9	0.763	0.765	0.778	0.728	0.662	0.688	0.561	0.692	0.714	0.105	0.44207	0.063153	8.5048	4.01E-08***
10	0.790	0.746	1.433	0.889	0.849	0.797	0.823	0.816	0.870	0.558	3.4409	0.49156	1.6488	0.1306
11	0.607	0.571	1.102	0.646	0.571	0.549	0.463	0.562	0.623	0.433	2.5614	0.36591	2.0975	0.05066
12	0.327	0.340	0.626	0.336	0.319	0.326	0.324	0.288	0.355	0.261	0.7319	0.104553	1.591	0.1468
13	0.733	0.637	0.564	0.762	0.720	0.694	0.848	0.592	0.702	0.630	0.726	0.10377	0.2482	0.9717
14	0.140	0.171	0.117	0.135	0.166	0.216	0.323	0.294	0.182	0.127	0.42461	0.060659	4.709	0.0001359***
15	0.337	0.378	0.273	0.345	0.429	0.548	0.839	0.836	0.450	0.336	3.4588	0.49411	5.7317	1.39E-05***
16	0.110	0.123	0.118	0.121	0.129	0.178	0.268	0.240	0.149	0.108	0.28046	0.040066	4.1151	0.000524***
17	1.270	1.098	1.092	1.112	1.171	1.112	1.213	1.494	1.145	0.146	0.84943	0.121348	8.5648	3.55E-08***
18	0.080	0.114	0.131	0.144	0.157	0.169	0.257	0.142	0.148	0.060	0.19747	0.0282103	15.383	1.74E-13***
19	0.103	0.126	0.144	0.158	0.183	0.190	0.310	0.206	0.170	0.075	0.32911	0.047016	17.165	1.08E-14***
20	1.123	0.928	0.904	0.939	0.921	0.872	0.841	1.218	0.933	0.135	0.66033	0.094333	7.2949	4.81E-07***
21	0.880	0.846	0.832	0.851	0.788	0.787	0.693	0.814	0.819	0.093	0.275	0.039285	6.0792	6.48E-06***
22	0.093	0.137	0.158	0.172	0.202	0.216	0.390	0.174	0.189	0.106	0.6209	0.0887	15.634	1.17E-13***
23	0.100	0.135	0.167	0.157	0.178	0.166	0.149	0.126	0.150	0.034	0.029793	0.0042562	4.6302	0.0001624***
24	0.130	0.122	0.107	0.115	0.127	0.134	0.358	0.162	0.149	0.176	0.60631	0.086616	3.2025	0.004232**
25	0.137	0.164	0.183	0.247	0.222	0.323	0.634	0.390	0.270	0.269	2.1855	0.312221	5.6335	1.72E-05***
26	0.170	0.230	0.251	0.362	0.314	0.396	0.512	0.568	0.335	0.175	1.1799	0.168551	8.1129	8.87E-08***
27	0.150	0.189	0.169	0.198	0.206	0.186	0.205	0.166	0.191	0.055	0.01885	0.0026928	0.9003	0.5095
28	0.530	0.417	0.423	0.441	0.401	0.666	1.712	0.946	0.617	0.909	17.851	2.5502	3.6235	0.001614*
29	1.560	1.289	0.957	0.859	1.043	0.913	1.311	0.996	1.085	0.433	4.5297	0.6471	4.1628	0.0004699***
30	2.090	1.704	1.382	1.300	1.442	1.579	3.024	1.942	1.701	1.270	28.221	4.0316	2.7976	0.01065*
31	0.310	0.364	0.393	0.358	0.433	0.420	0.482	0.368	0.387	0.078	0.1983	0.0283284	6.3666	3.47E-06***
32	0.617	0.615	0.591	0.594	0.546	0.593	0.572	0.530	0.591	0.043	0.060826	0.0086895	6.409	3.17E-06***
33	1.647	1.625	1.476	1.475	1.420	1.621	1.467	1.182	1.515	0.274	1.2413	0.177322	2.6097	0.01628*
34	0.057	0.049	0.044	0.059	0.058	0.060	0.088	0.066	0.058	0.025	0.015091	0.00215587	4.3552	0.0003032***
35	0.063	0.075	0.079	0.086	0.113	0.099	0.117	0.082	0.088	0.022	0.024423	0.003489	13.886	2.03E-12***
36	1.400	1.305	1.229	1.178	1.160	1.271	1.183	1.048	1.225	0.191	0.5843	0.083466	2.5263	0.01963*
37	0.427	0.431	0.431	0.448	0.436	0.432	0.476	0.438	0.441	0.062	0.02172	0.0031026	0.7876	0.5993
38	1.150	1.048	1.032	1.119	1.288	1.096	1.043	1.410	1.110	0.158	0.96524	0.137891	8.0702	9.68E-08***
39	0.837	0.773	0.830	0.766	0.761	0.813	0.783	0.414	0.764	0.106	0.69634	0.099477	19.965	<2.20E-16***
40	0.337	0.325	0.338	0.355	0.326	0.309	0.333	0.408	0.338	0.054	0.047962	0.0068517	2.5897	0.01703*
41	0.553	0.604	0.647	0.621	0.618	0.640	0.609	0.590	0.615	0.100	0.03415	0.0048789	0.474	0.8513
42	0.047	0.053	0.060	0.060	0.064	0.062	0.074	0.056	0.060	0.013	0.0046989	0.00067128	4.8558	9.76E-05***

TABLE 4. Continued

Index No.	Mean of each locomotor mode								Total Mean	Sd	Multivariate ANOVA Test			
	G	A	Sc	T	Sa	Sf	F	S			Sum Square	Mean Square	*F*-value	Pr (>F)
43	0.020	0.032	0.029	0.029	0.030	0.034	0.042	0.014	0.031	0.018	0.0034658	0.00049511	1.606	0.1425
44	0.260	0.289	0.277	0.276	0.250	0.324	0.269	0.204	0.277	0.139	0.05964	0.0085202	0.4213	0.887
45	0.630	0.581	0.804	0.687	0.728	0.631	0.569	0.642	0.649	0.242	0.5374	0.076773	1.3351	0.2419
46	0.077	0.122	0.108	0.107	0.128	0.118	0.153	0.070	0.116	0.045	0.036663	0.0052376	2.8421	0.009624**
47	0.047	0.065	0.074	0.070	0.083	0.070	0.084	0.044	0.070	0.024	0.010041	0.00143445	2.6925	0.01351*
48	0.483	0.501	0.428	0.454	0.457	0.452	0.467	0.452	0.467	0.076	0.05818	0.0083118	1.4828	0.1821
49	0.697	0.713	0.722	0.770	0.690	0.752	0.728	0.902	0.741	0.180	0.2133	0.030475	0.938	0.4809
50	0.380	0.392	0.324	0.368	0.342	0.361	0.294	0.274	0.356	0.071	0.13533	0.0193334	4.7702	0.0001184***
51	0.337	0.350	0.399	0.404	0.403	0.368	0.471	0.518	0.396	0.087	0.22423	0.032033	5.555	2.05E-05***
52	1.137	1.238	0.880	0.956	0.891	1.012	0.640	0.546	0.979	0.447	4.5866	0.65522	3.9184	0.0008214***
53	0.733	0.807	0.598	0.655	0.688	0.656	0.779	0.724	0.715	0.235	0.5779	0.082561	1.5461	0.1607
54	0.300	0.284	0.330	0.293	0.296	0.332	0.294	0.274	0.297	0.062	0.02911	0.0041583	1.1004	0.3689
55	0.767	0.947	0.888	0.954	0.959	0.914	1.014	0.972	0.946	0.187	0.1984	0.028343	0.7959	0.5925
56	0.227	0.264	0.288	0.270	0.283	0.301	0.280	0.254	0.273	0.041	0.021511	0.003073	1.9056	0.0765

*$p < 0.1$, **$p < 0.01$, ***$p < 0.001$

At the opposite extreme, fossorial mammals possess the most robustly built postcranial skeletons of the eight locomotor modes. They tend to have (i) an enlarged scapula (SI), (ii) a robust and longer forelimb with a prominent humeral deltopectoral crest and a relatively wide humeral distal end (HEB, HRI, and DI), (iii) an ulna with an enlarged olecranon process (OPLI), (iv) a robust hand with shortened proximal and intermediate phalanges and elongate distal phalanges (PPRI, IPRI, PI, and MRTI), (v) a shortened ilium (IRI), (vi) a robust femur with an elevated greater trochanter (FRI and GI), (vii) a shortened and robustly built tibia and fibula (TRI), (viii) a reduced astragalar neck and calcaneal body (CBRI), and (ix) an elongate calcaneal tuber (CTRI). Semi-fossorial mammals have similar morphological signatures but to a lesser degree and without the reduction of the ilium found in fossorial taxa. Semiaquatic mammals also tend to be robustly built, having (i) an anteroposteriorly compressed scapula (SI), (ii) a robust humerus with bilaterally expanded proximal and distal ends (HEB, HRI, and Hpw:Hl; see Table 3 for definition), (iii) a well-developed humeral deltopectoral crest (DI), (iv) an enlarged hand (MRTI), (v) a shortened ilium (IRI), (vi) a robust hind limb with a pronounced greater trochanter of the femur (FRI, GI, and TRI), and (vii) an elongate tibia and fibula (CI).

Distinct from all other locomotor modes, saltatorial mammals mainly travel by bipedal hopping and are characterized by (i) a greatly reduced forelimb and an elongated hind limb (IM), (ii) gracile limb elements (HRI, FRI, and TRI), (iii) a relatively shortened humerus (BI), (iv) a relatively large hand (MRTI), (v) a shortened ilium (IRI), (vi) a poorly developed greater trochanter of the femur (GI), (vii) a shortened calcaneal body (CBRI), and (viii) an elongate calcaneal tuber (CTRI).

Predicted Locomotor Modes of Small-bodied Extant Mammals

Eight-Locomotor-Mode Analysis.—This CVA included all locomotor modes in our data set (Fig. 4A, Supplementary Fig. 1A). Together, the first three canonical functions (CFs) account for 85.50% of the variance in the data set

TABLE 5. Morphological signatures of each locomotor mode. Abbreviations: G, gliding; A, arboreal; F, fossorial; S, saltatorial; Sc, scansorial; Sa, semiaquatic; Sf, semifossorial; T, terrestrial. Symbols: ++, relatively robust; +, relatively large, long, or wide; -, relatively small, short, or slender; --, relatively very small or extremely gracile; ==, equal; =, intermediate; *, varies; fd, forelimb dominated; hd, hind limb dominated.

	Locomotor mode							
Morphological signature	G	A	Sc	T	Sa	Sf	F	S
Scapular length	+	-	*	+	+	*	*	-
Deltopectoral crest width	--	-	-	*	+	+	++	-
Olecranon process length	--	-	-	*	+	+	++	-
Palm size	-	-	*	+	-	*	--	-
Proximal and intermediate phalangeal length	-	-	*	+	-	*	--	-
Distal phalangeal robustness	-	-	-	-	+	*	++	+
Ilium length	+	+	=	*	-	+	-	-
Greater trochanter length	-	-	-	*	+	+	++	-
Forelimb robustness	--	-	*	*	+	+	++	-
Hind limb robustness	--	-	*	*	+	+	++	-
Limb use domination	fd	==	fd	==	*	*	fd	hd

(CF1 = 49.13%, CF2 = 25.83%, CF3 = 10.54%; Supplementary Table 3). In the morphospace formed by the CF1 vs. CF2 scores, the gliding, fossorial, and saltatorial mammals are well separated from each other and the remaining locomotor modes. Their centroids are at the extremes of the morphospace. In contrast, the remaining five locomotor modes overlap in the morphospace and their centroids are clustered near the origin. The morphological variance of each locomotor mode shows that gliding taxa have the smallest variance, followed by scansorial, arboreal, terrestrial, saltatorial, semiaquatic, semifossorial, and fossorial taxa (Fig. 4C, Supplementary Table 4).

CF1 is strongly positively correlated with Ul:Hl (see Table 3 for definition), the brachial index (BI), and the crural index (CI), and negatively correlated with the Intermembral (IM) indices (Fig. 4B, Supplementary Fig. 1B). The saltatorial species are well separated from other modes along CF1 due to a high CI and a low IM (high CF1 scores). CF2 is negatively correlated with numerous robustness, morpho-functional, and proportional indices of the forelimb, which separates the fossorial, semi-fossorial, and saltatorial mammals from other modes in the morphospace. These indices include Sl:Hl (see Table 3 for definition), the humeral robustness index (HRI), the humeral proximal robustness index (HPEI), the humeral epicondylar index (HEB), Hsw:Hpw (see Table 3 for definition), the humeral head robustness index (HHRI), Hdcw:Hpw, the deltopectoral index (DI), Hdcw:Hdw, the olecranon process length index (OPLI), Uol:Hl, Uol:Rl (see Table 3 for definition), the robustness index of proximal and intermediate phalanges (PPRI and IPRI), and the manual robustness index (MRTI), as well as a few hind limb indices, such as the gluteal index (GI), the femoral robustness index (FRI), the calcaneal tuber robustness index (CTRI). CF2 is positively correlated with HHw:Hpw, Rl:Ul (see Table 3 for definition), the ilia robustness index (IRI), and the calcaneal body robustness index (CBRI) (Fig. 4B). CF3 is negatively correlated with HRI, three deltopectoral-crest-related indices, OPLI, the phalangeal index (PI), and GI, and positively correlated with the palm robustness index (PRTI) (Supplementary Fig. 1B). CF3 successfully separates scansorial and terrestrial mammals from fossorial and saltatorial mammals.

The CVA correctly classified 89.72% of the individuals (100% of gliding, semifossorial, and saltatorial taxa; 93.93% of arboreal taxa; 88.89% of scansorial and semiaquatic taxa; 86.67% of terrestrial taxa; and 75.00% of fossorial taxa). In total, 11 of 107 species were misclassified (Supplementary Table 5) and the majority of misclassified taxa are from arboreal, scansorial, terrestrial, and semifossorial locomotor modes.

Five-Locomotor-Mode Analysis.—Removing the gliding, fossorial, and saltatorial modes from the CVA improved the segregation of the remaining five locomotor modes (Supplementary Fig. 2A, C). The first three CFs accounted for 93.36% of the variance

(CF1 = 48.30%, CF2 = 27.61%, CF3 = 17.45%; Supplementary Table 6). In the plot of CF1 vs. CF2 (Supplementary Fig. 2A), the locomotor modes appear to be separated farther apart, relative to the distribution of these modes in the eight-locomotor-mode analysis. Although the arboreal, terrestrial, semifossorial, and semiaquatic modes are well separated from

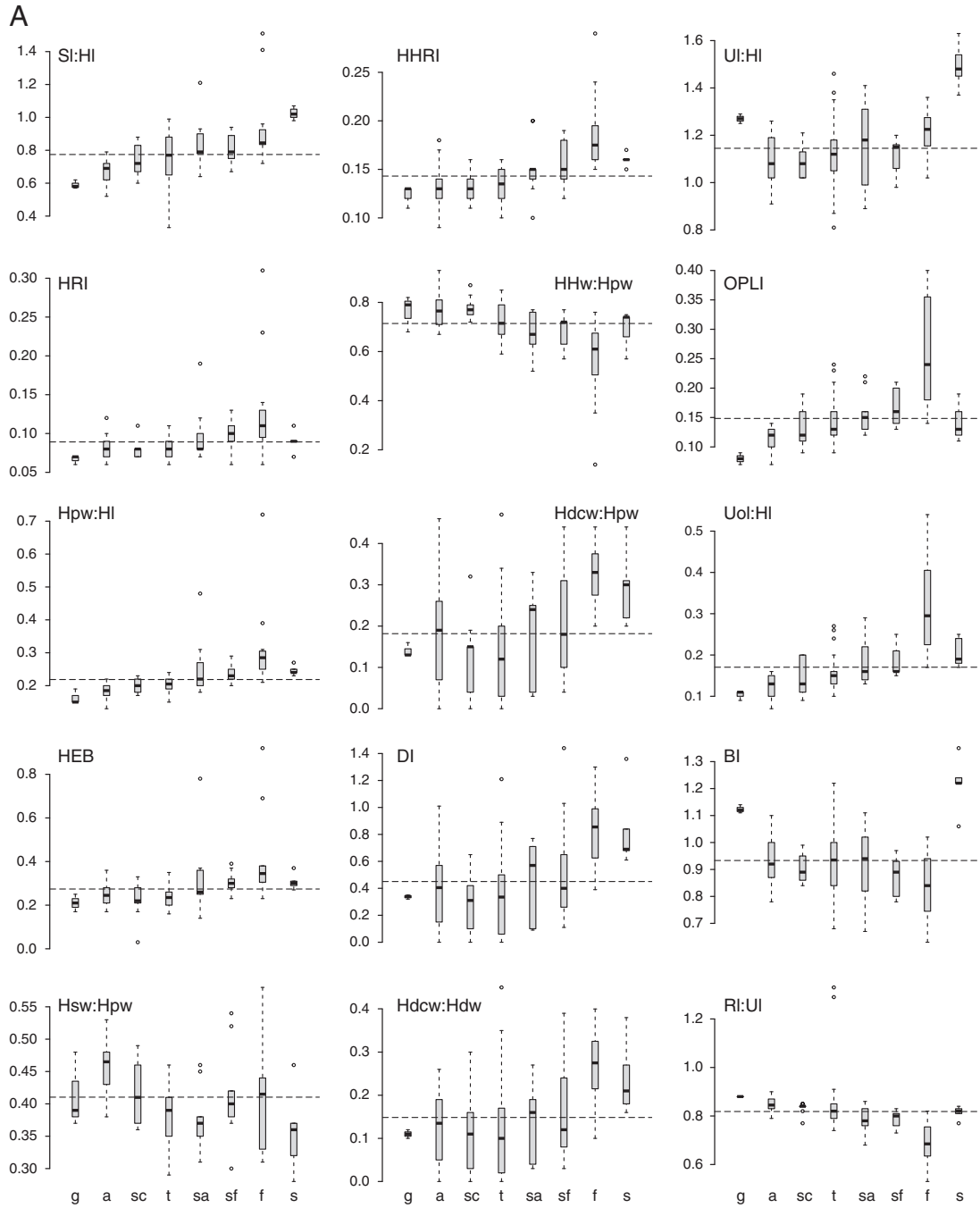

FIGURE 3. A, B. Boxplots of 30 osteological indices for our extant small-bodied mammal data set. Abbreviations: g, gliding; a, arboreal; sc, scansorial; t, terrestrial; sa, semiaquatic; sf, semifossorial; f, fossorial; s, saltatorial. See descriptions of the osteological indices in Table 3.

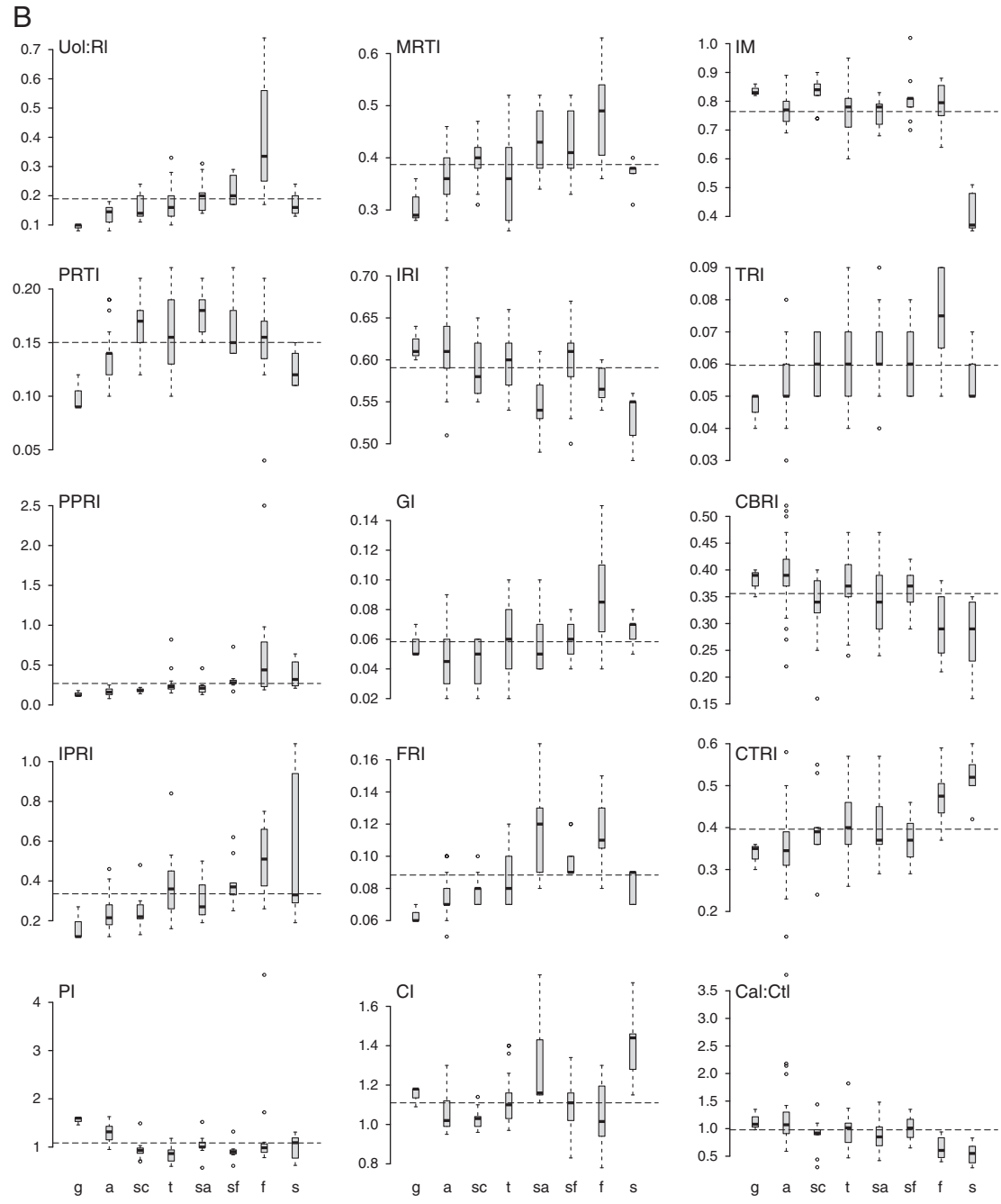

FIGURE 3. Continued.

each other, the scansorial mode still overlaps with the arboreal and terrestrial modes.

In the structure matrix, the structure coefficients indicate that CF1 is highly correlated with two robustness and two morphofunctional indices: the olecranon process length index (OPLI), the proximal phalangeal robustness index (PPRI), the intermediate phalangeal robustness index (IPRI), and the phalangeal index (PI) (Supplementary Table 6). These four indices are also highly correlated with CF2 and CF3, suggesting that they play a significant role

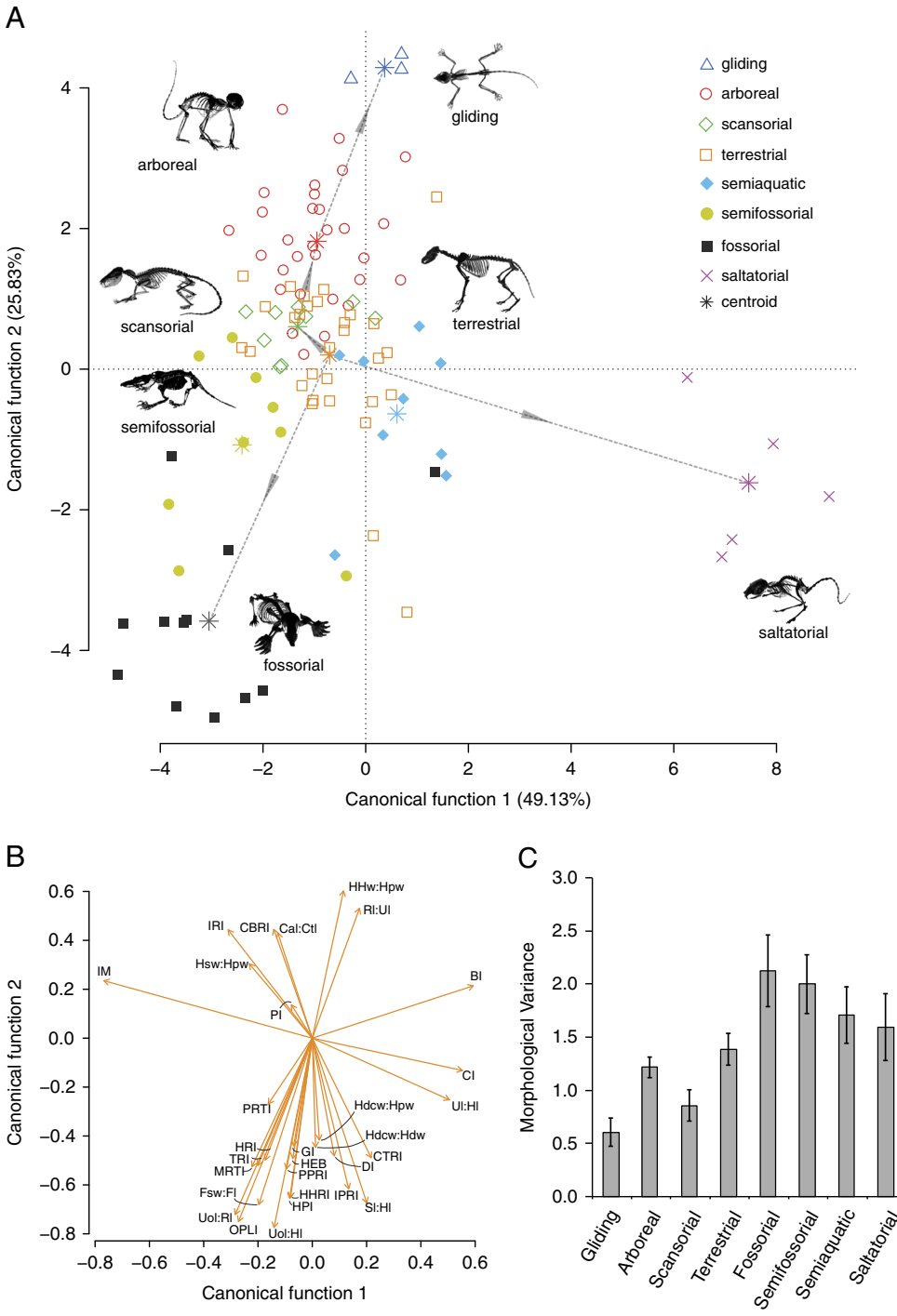

FIGURE 4. Ordination of locomotor modes of small-bodied extant mammals in the eight-locomotor-mode analysis. A, Plot of canonical functions (CF) 1 and 2 from the canonical variate analysis (CVA). Dashed lines with arrows show axes of morphofunctional continua among locomotor modes. B, Plot of structure correlations between the osteological indices and the CF1 and CF2. C, Morphological variances among eight locomotor modes. The morphological variance is calculated by using the mean of the distances between species in a locomotor mode and their corresponding centroid, using first three CF scores in each locomotor mode.

in segregating among the five locomotor modes. On CF1, the semifossorial taxa have high scores and are well separated from the other four taxa. Most of the semiaquatic taxa have very low CF1 scores and separate themselves from the other four locomotor modes. Together, the five locomotor modes form a morphological gradient along CF1, from semiaquatic to arboreal/scansorial/terrestrial and semifossorial modes (Supplementary Fig. 2A,C).

Along CF2, the morphological gradient extends from semiaquatic to semifossorial, terrestrial, and arboreal/scansorial modes (Supplementary Fig. 2A). Each locomotor mode overlaps to varying degrees with the adjacent locomotor modes. CF2 is correlated with numerous indices as well as the four osteological indices that were strongly correlated with CF1 (Supplementary Table 6, Supplementary Fig. 2B). It is negatively correlated with Sl:Hl, the humeral robustness index (HRI), the humeral proximal end robustness index (HPEI), the humeral epicondylar index (HEB), Hsw:Hpw, the humeral head robustness index (HHRI), HHw:Hpw, Uol:Hl, Uol:Rl, the palm robustness index (PRTI), the manual robustness index (MRTI), the femoral robustness index (FRI), and the tibial robustness index (TRI), and positively correlated with HHw:Hpw and the ilium robustness index (IRI).

CF3 is negatively correlated with Hsw:Hpw, the calcaneal body robustness index (CBRI), and Cal:Ctl (see Table 3 for definition), and positively correlated with the olecranon process length index (OPLI) and calcaneal tuber robustness index (CTRI) (Supplementary Table 6, Supplementary Fig. 2D). CF3 segregates the five locomotor modes into three groups, from arboreal to semiaquatic/semifossorial and scansorial/terrestrial (Supplementary Fig. 2C).

The CVA correctly classified 95.40% of the individuals (100% of semifossorial, 96.67% of arboreal, 96.67% of terrestrial, 88.89% of scansorial, and 88.89% of semiaquatic). Four of the 11 species that were misclassified in the eight-locomotor-mode analysis remain misclassified here (Supplementary Table 7).

Three-Locomotor-Mode Analysis.—To further understand the morphological differences among arboreal, scansorial, and terrestrial taxa, we removed all other locomotor modes from the CVA. The results indicate that two canonical functions account for 100% of variance in the data set (Supplementary Table 8). The plot of CF1 vs. CF2 shows unambiguous segregation of the three locomotor modes (Supplementary Fig. 3).

CF1 accounts for 55.93% of the variance and separates the three locomotor modes into three discrete groups in the morphospace (Supplementary Fig. 3A). The scansorial mode plots intermediate between the arboreal and terrestrial modes. Given the structure matrix, CF1 positively correlates with Sl:Hl, the humeral proximal end index (HPI), the olecranon process index (OPLI), Uol:Hl, Uol:Rl, the palm robustness index (PRTI), the proximal phalangeal robustness index (PPRI), the intermediate phalangeal robustness index (IPRI), the femoral robustness index (FRI), the crural index (CI), the tibial robustness index (TRI), and the calcaneal tuber robustness index (CTRI), and negatively correlates with Hsw:Hpw, HHw:Hpw, the phalangeal index (PI), and the Cal:Ctl (Supplementary Table 8, Supplementary Fig. 3B). CF2, which accounts for the remaining 44.07% of the variance, separates the scansorial mode from the arboreal/terrestrial modes. It negatively correlates with the palm robustness index (PRI), intermembral index (IM), and positively correlates with calcaneal body robustness index (CBRI) (Supplementary Table 8, Supplementary Fig. 3B).

The CVA correctly classified 97.10% of the individuals (100% of terrestrial, 96.67% of arboreal, and 88.89% of scansorial taxa; Supplementary Table 9). The only misclassified taxa are *Rattus andamanensis* and *Heliosciurus rufobrachium*, which were also misclassified in the five- and eight-locomotor-mode analyses.

Predicted Locomotor Mode of Mesozoic Mammals

We used the above CVAs of extant small-bodied mammals as a framework for inferring the locomotor mode of ten Mesozoic mammal species that are known from relatively complete postcranial skeletons. The results of the eight-locomotor-mode analysis indicate that *Fruitafossor*, *Repenomamus*, and *Liaoconodon* were likely adapted for fossorial, semifossorial, and semiaquatic lifestyles, respectively, given the 100% posterior probabilities. Our analysis also yielded high posterior probabilities (>95%)

for *Rugosodon*, *Jeholodens*, *Yanoconodon*, and *Akidolestes* as arboreal, arboreal, semiaquatic, and semifossorial mammals, respectively. The locomotor inferences for *Haldanodon* were ranked in order of decreasing posterior probability, as follows (Table 1): arboreal (56.6%), semifossorial (41.6%), and terrestrial (1.8%), suggesting that this analysis cannot clearly determine whether this taxon is arboreal or semifossorial. For *Eomaia*, the posterior probabilities of the locomotor inferences were ranked as follows: arboreal (68.6%), scansorial (16.5%), and terrestrial (11.3%), whereas for *Zhangheotherium*, the posterior probabilities were ranked from semifossorial (32.6%), to scansorial (26.2%), arboreal (20.0%), and terrestrial (11.6%), suggesting that the locomotor modes of *Eomaia* and *Zhangheotherium* cannot not be determined by an eight-locomotor-model analysis.

The results of the five-locomotor-mode analysis, supported by high posterior probabilities, indicate that *Haldanodon* (100%) and *Eomaia* (93.2%) are likely semifossorial and arboreal mammals, respectively. The results also suggest that *Rugosodon* (94.8%) and *Zhangheotherium* (71.25%) were both scansorial mammals rather than arboreal as inferred by the eight-locomotor-mode analysis. Moreover, the results indicate that *Jeholodens* had some morphological features that are adapted to terrestrial locomotion (21.2%). The inferred locomotor adaptations of *Yanoconodon*, *Liaoconodon*, and *Akidolestes* from the five-locomotor-mode analysis are consistent with the inferences from the eight-locomotor-mode analysis (semiaquatic, semiaquatic, and semifossorial, respectively).

Discussion

The Link between Postcranial Morphology and Locomotor Mode in Extant Small-Bodied Mammals

Different locomotor modes place different mechanical and energetic demands on the appendicular skeleton of vertebrates (Tucker 1970, 1975; Hildebrand et al. 1985; Biewener 1989, 1990, 2003). Adaptation to these demands is associated with morphological modifications. These modifications tend to be pronounced in mammals, which have higher metabolic requirements and thus greater need for efficient movement across the landscape than do most other vertebrates (McNab 2002). Because total energetic costs of locomotion scale with body size (see McNab 1990; Biewener 2003), larger-bodied mammals would seem to have higher selective pressures than small-bodied mammals, presumably resulting in distinct morphological adaptations to locomotor mode. Moreover, preservation bias and collecting methods favor recovery of larger skeletal elements in the fossil record. For these reasons, paleontologists have tended to focus on inferring locomotor mode in large-bodied fossil mammals over small-bodied ones, quantitatively establishing the link between postcranial morphology and locomotion by using extant analogues (Van Valkenburgh 1987; Janis et al. 2002; Polly 2008, 2011; Bassarova et al. 2009; Samuels et al. 2013). The underlying assumption is that in small-bodied mammals this link would be subtle or indistinguishable and that scansoriality is an obligatory locomotion in small-bodied mammals (Jenkins 1974; Jenkins and Parrington 1976). However, multiple studies have shown that the same biomechanical selective forces operate on both small- and large-bodied mammals (Szalay 1984; Sargis 2001b; Szalay and Sargis 2001). Nonetheless, few studies have attempted to quantitatively infer locomotion in smaller-bodied fossil mammals (but see Samuels and Van Valkenburgh 2008; Hopkins and Davis 2009). Here, we tested this assumption by attempting to establish a link between postcranial morphology and locomotor mode in a sample of small-bodied extant mammals of diverse locomotor modes and phylogenetic histories, using multivariate analysis of morphometric data from postcranial skeletons.

The results from our multivariate analyses show that the link between postcranial morphology and locomotor mode in small-bodied mammals is indeed subtle but detectable. The eight-locomotor-mode analysis segregated the most specialized locomotor groups (gliding, fossorial, and saltatorial), leaving the remaining locomotor groups (arboreal, scansorial, terrestrial, semiaquatic, and semifossorial) in a cluster (Fig. 4A, Supplementary Fig. 1A). Despite this clustering, the CVA correctly classified nearly 90% of the extant taxa into their

correct locomotor modes. A secondary analysis (five-locomotor-mode analysis), which excluded the most specialized locomotor groups, further segregated the semifossorial and semiaquatic groups from the main cluster of terrestrial, arboreal, and scansorial taxa (Supplementary Fig. 2A,C). Prediction of locomotor group membership improved to better than 95% in this analysis. The cluster of terrestrial, scansorial, and arboreal taxa persisted, but this is not surprising in light of variable definitions of scansoriality and variable assignment of extant taxa to these modes in the literature (Kingdon 1997; Iwaniuk et al. 1999; Nakagawa et al. 2007; Kelt and Meyer 2009; Shattuck and Williams 2010; Chen and Luo 2013). Moreover, an individual mammal's perception of its substrate likely scales with body size (but see Szalay and Sargis 2001); for example, during ground locomotion across uneven substrate, some small-bodied terrestrial mammals, such as an island mouse (*Nesomys rufus*), might require a degree of climbing, whereas large-bodied mammals, such as a red fox (*Vulpes vulpes*), can cross the same substrate without climbing. This phenomenon can further blur formal distinctions among locomotor modes. Nevertheless, in our third analysis (three-locomotor-mode analysis), the terrestrial, scansorial, and arboreal modes were fully separated from each other (Supplementary Fig. 3A) and over 97% of the sampled taxa were correctly classified to their respective locomotor mode. Taken together, these results provide promise for inferring locomotion in small-bodied fossil mammals. The most specialized locomotor modes (gliding, fossorial, and saltatorial) have very distinctive postcranial morphologies that are readily detectable in our eight-locomotor-mode analysis, and the more subtle morphological differences among less specialized groups become perceptible as specialized modes are progressively removed from the analyses (five-locomotor-mode and then three-locomotor-mode analyses).

The large morphological variance *within* locomotor modes contributes to the difficulty in distinguishing *among* locomotor modes. This morphological variance stems from phylogenetic and functional diversity in our data set. By design, we sampled a phylogenetically broad range of taxa for each locomotor mode in hopes that our analyses would detect a robust signal of functional adaptations rather than a narrow subset of shared derived features (synapomorphies). Our results show that this approach was successful. At a higher taxonomic level, our analysis accurately segregated the large samples of marsupials, carnivorans, and rodents according to locomotor mode not phylogeny (Fig. 5), a result that is consistent with previous studies (Van Valkenburgh 1987; Iwaniuk et al. 1999; Weisbecker and Warton 2006; Weisbecker and Schmid 2007; Samuels and Van Valkenburgh 2008; Bassarova et al. 2009; Samuels et al. 2013). The merit of this approach extends to the subgenus level, where, for example, four species of *Tupaia* (*T. longipes* and *T. tana* [both terrestrial], *T. glis* [scansorial], and *T. minor* [arboreal]) were segregated in the ecomorphospace according to their locomotor modes (Fig. 5). A trade-off of having phylogenetic diversity within locomotor-mode samples is the associated increase in morphological diversity that results from divergent evolutionary histories. Although this variance inherently limits our ability to distinguish among locomotor modes relative to more phylogenetically uniform samples (e.g., a fossorial group of only rodents), it enables robust locomotor inference for a phylogenetically broader range of extinct taxa.

Additional morphological variance results from functional diversity within locomotor modes, most notably within the fossorial, semifossorial, and semiaquatic samples (Fig. 4C). Fossorial and semifossorial samples include taxa that employ diverse digging modes, from chisel-tooth, to scratch, head-lift, humeral-rotation, and combinations thereof (Hildebrand 1985; Hildebrand and Goslow 1998; Stein 2000; Hopkins and Davis 2009). Likewise, some semiaquatic mammals emphasize forelimb propulsion (e.g., *Neovison vison* in surface swimming [Dunstone 1979]), whereas others (e.g., *Chironectes minimus* [Howell 1930; Marshall 1978] and *Ondatra zibethicus* [Fish 1993]) emphasize hind limb propulsive paddling. In turn, the associated postcranial adaptations of these taxa within the same locomotor mode can vary substantially (e.g., humeral-rotation diggers tend to have a more bilaterally expanded humerus than scratch diggers). Inclusion of this functional diversity in our data set dilutes the

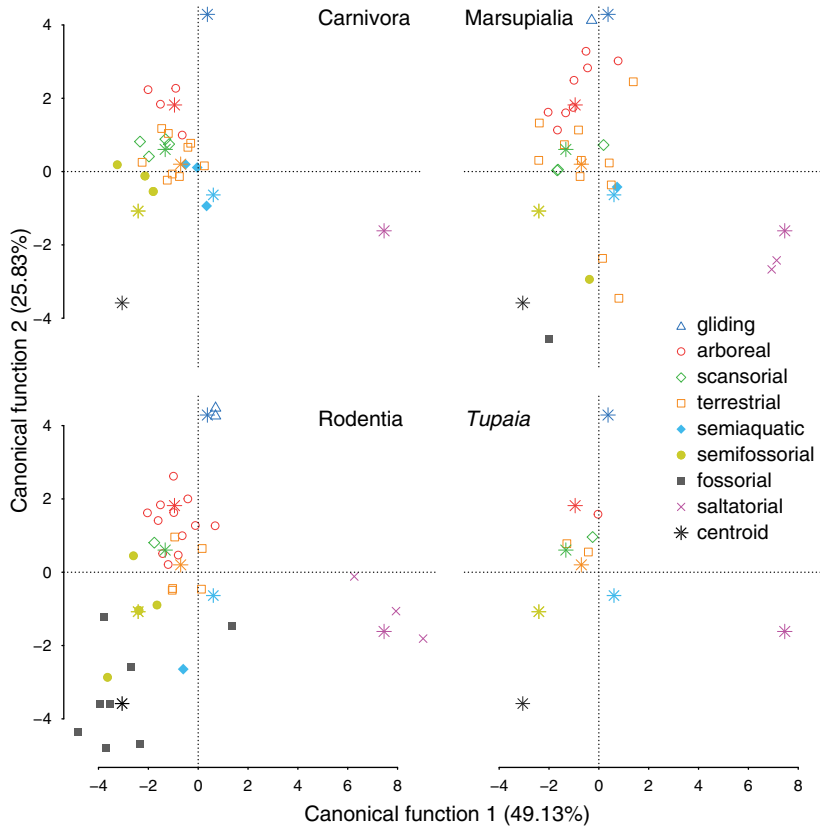

FIGURE 5. CVA plots (first two functions) of eight-locomotor-mode analyses for Carnivora, Rodentia, Marsupialia, and *Tupaia*. Rodents use eight locomotor modes, whereas marsupials and carnivorans use six and four locomotor modes, respectively. Species of the genus *Tupaia* use arboreal, scansorial, and terrestrial locomotor modes. The centroids represent the centroids of the full dataset.

morphological signal of any one locomotor mode (i.e., makes it less uniform), but it better reflects the reality among extant small-bodied mammals and improves our ability to capture locomotor diversity in fossil taxa. The saltatorial mode also exhibits large morphological variance, but for a different reason. Saltatorial taxa commonly show a striking elongation of their hind limbs for bipedal hopping, whereas their forelimbs are only minimally involved in locomotion. As a result, the forelimbs of saltatorial taxa often evolve for other activities (e.g., food manipulation, digging). This evolutionary independence of the forelimb not only increases the morphological variance in this group, but it can also complicate locomotor inferences. For example, several saltatorial taxa (e.g., *Potorous tridactylus*, *Aepyprymnus rufescens*, *Jaculus jaculus*) exhibit forelimb adaptations associated with scratch digging, which if analyzed without hind limb indices would lead to their classification as members of the semifossorial group. This result highlights the importance of analyzing an anatomically broad set of indices rather than a few that focus on select anatomical elements (e.g., only the forelimb) whenever possible; however, we acknowledge that small-bodied mammal fossils are typically less complete than those in our sample. Moreover, it should be noted that the accuracy of locomotor predictions using our multivariate approach decreases as the number of available postcranial measurements decreases.

A couple of caveats to future application of this morphometric approach should be noted. First, allometric scaling has profound influence on morphological and ecological adaptation of mammals. It may produce major differences

between large- and small-bodied mammals in their morphological adaptation to the same locomotor mode (e.g., the arboreal marsupial *Caluromys* versus the arboreal primate *Hylobates*; McMahon 1975; Alexander 1985). Thus, for robust locomotor inference of extinct taxa, the analogue extant species in the morphometric data set should be of comparable body size to the fossil taxa. Second, the coverage of locomotor modes in the morphometric data set also affects locomotor inference of extinct mammals. For example, inclusion of too many locomotor modes in the morphometric data set, especially highly specialized ones like fossorial and saltatorial modes, could result in poor segregation of locomotor modes in the ecomorphospace plots (although prediction error may still be low). In contrast, incomplete coverage of locomotor modes in the morphometric data set could in some cases lead to inaccurate locomotor prediction of extinct mammals. Thus, the composition of the analogue extant taxa in the morphometric data set should be carefully chosen based on initial morphological assessment of the fossil taxon. For example, if the fossil taxon lacks the obvious morphological signatures associated with gliding, the effectiveness of the analysis to discriminate among the non-gliding modes for this taxon would be improved by removal of gliders from the morphometric data set, thus improving the inferential power of the analysis. In sum, the morphometric data set of extant taxa and the analyses should be tailored to the fossil taxa of interest whenever possible.

Morphofunctional Continuum among Locomotor Modes

The eight locomotor modes in our analyses not only possess distinct postcranial morphologies but also ordinate in the ecomorphospace (Fig. 4A, Supplementary Fig. 1A) according to shared biomechanical properties. In the eight-locomotor-mode analysis, CF1 segregates locomotor modes by forelimb to hind limb proportions, i.e., facultative bipeds (saltatorial) versus quadrupeds (all other modes). CF2 generally ordinates locomotor modes according to mechanical advantage. Modes that emphasize force over speed (fossorial, semifossorial, semiaquatic) have robustly built appendicular skeletons and short output levers (low CF2 scores), whereas modes that emphasize speed over force (gliding, arboreal) have more gracile appendicular skeletons and long output levers (high CF2 scores). The saltatorial mode is the exception to this pattern. Despite having hind limb adaptations for bipedal hopping (speed), several saltatorial taxa have forelimb adaptations for digging (force) that lead to low CF2 scores, comparable to other modes that emphasize the strength and magnitude of output forces, such as fossorial, semifossorial, and semiaquatic.

Within this morphofunctional continuum of locomotor modes, the terrestrial mode lies near the origin (Fig. 4A, Supplementary Fig. 1A). As morphological features become progressively more gracile (increasing CF2 scores), the continuum extends from the terrestrial mode to the scansorial, arboreal, and gliding modes. The decreasing robustness of postcranial elements reduces body mass, which is generally correlated with increased flexibility of skeletal elements and joints of these mammals. This enhances the dexterity and precision of movement in mammals that move among trees, simultaneously mitigating the risk of falling during climbing. The scansorial mode is intermediate between terrestrial and arboreal modes (Fig. 4A, Supplementary Figs. 2A, 3A) and shares numerous morphological features with these other modes. The only distinctive morphological feature of the scansorial mode is a more elongate forelimb (high IM) than that of terrestrial and arboreal taxa. This forelimb elongation suggests that scansorial taxa have more forelimb-dominated locomotion than the arboreal and terrestrial taxa. This would functionally correlate with the ability of scansorial mammals to ascend and descend (Polly 2007). In the arboreal mode, the postcranial elements are even more slender and exhibit greater reduction of crests and tubercles than in the scansorial and terrestrial modes. The latter modification enables greater mobility at the joints, thereby increasing agility for arboreal locomotion (Cartmill 1985; Argot 2001, 2002; Sargis 2001a, 2002a,b). Relative to scansorial and terrestrial modes, arboreal taxa also have more elongate digits and smaller palms (high PI and low PRTI, respectively), both of

which correlate with prehensility (Jouffroy and Lessertisseur 1979; Cartmill 1985; Van Valkenburgh 1987; Jouffroy et al. 1993; Lemelin 1999; Argot 2001, 2002; Sargis 2001a, 2002a,b; Bloch and Boyer 2002; Weisbecker and Warton 2006; Kirk et al. 2008; Weisbecker and Schmid 2007; Boyer et al. 2013). In the gliding mode, the appendicular skeleton is exceptionally gracile and lacks prominent crests and tubercles. These modifications further reduce body mass and further increase joint mobility for gliding locomotion (Samuels and Van Valkenburgh 2008).

In the opposite direction, the morphofunctional continuum extends from the terrestrial mode to the semiaquatic/semifossorial and fossorial modes with morphological features becoming progressively more robust (decreasing CF2 scores) (Fig. 4A). This aspect of the continuum reflects the need to withstand the increasingly high mechanical stresses incurred in these locomotor modes (Lanyon and Rubin 1985; Biewener 1989). The trend toward increasingly more robust elements is coupled with a trend toward increasingly greater area for muscle attachment (e.g., high HRI, HPI, OPLI, MRTI, FRI, and TRI). The postcranial elements of fossorial taxa are the most robust of all locomotor modes. The semifossorial and semiaquatic modes are intermediate on this aspect of the continuum. However, separation along CF1 indicates important functional differences between semifossorial and semiaquatic modes. Relative to semiaquatic taxa, semifossorial taxa tend to have shorter limb output levers (e.g., less elongate radius, ulna and tibia [high BI and CI]) (Croft and Anderson 2008; Samuels and Van Valkenburgh 2008; Samuels et al. 2013). This slight morphological difference likely reflects the greater propulsive forces needed for a digging stroke against soil versus a swimming stroke against water. Moreover, within the semifossorial mode, the output lever of the forelimb is smaller than that of the hind limb (BI higher than CI), which indicates that power of the digging stroke in semifossorial (and fossorial) taxa resides in the forelimb rather than the hind limb. In contrast, the relative lengths of the ulna and tibia vary in semiaquatic taxa. This likely reflects differences in primary swimming strategies among semiaquatic taxa, from forelimb-, to hindlimb-, and all-limb-dominated modes. In fossorial taxa, postcranial elements are even more robust and the relative size of the manus is substantially larger than in the semifossorial and semiaquatic modes. These more extreme morphological adaptations (relative to semifossorial taxa) reflect a more subterranean existence, in which these animals often develop elaborate tunnel systems (Hildebrand 1985; Hildebrand and Goslow 1998; Stein 2000).

The morphofunctional continuum also extends from the terrestrial to saltatorial mode. Saltatorial taxa have forelimbs that are reduced relative to their elongate hind limbs (increasing CF1 scores) (Fig. 4A). This change in morphology relative to the terrestrial mode reflects a shift toward rapid and simultaneous extension of both hind limbs in bipedal hopping. Energetically, bipedal hopping is a more efficient mode of transportation over long distances than the seven other locomotor modes (McNab 2002). In saltatorial taxa, the ischium is elongate relative to the ilium (low IRI). Although this morphological change would seem to increase the input lever for the hip extensors, a proximal insertion of these muscles on the tibia only maintains the same input lever length relative to non-jumping mammals (Emerson 1985). Instead, the enlarged hip extensor muscles increase the output force during the propulsive stroke (Gambaryan 1974; Alexander et al. 1981; Emerson 1985). Moreover, the elongate tibia (high CI) results in a longer output lever of the hind limb musculature, thereby increasing the speed of the propulsive stroke. Together, these changes to the pelvis and hind limb optimize jumping ability in saltatorial taxa. In contrast, the forelimbs of three saltatorial taxa (*Potorous tridactylus*, *Aepyprymnus rufescens*, *Jaculus jaculus*) show adaptations for scratch digging. Despite slender elongate hind limbs (e.g., low FRI, TRI), the forelimbs of these three taxa are relatively robust with well-developed crests and tubercles (e.g., high HRI, HHRI, DI). These enlargements increase the attachment area for large muscles and the resistance against high stresses incurred during scratch digging. These changes of the forelimb are independent of those of the hind limbs. Their differences point to a modularity of development and a modularity in locomotor function between the forelimb and hind limb of

these saltatorial mammals. It is noteworthy that locomotor inferences based on only the forelimb or only the hind limb could be misleading.

Taken together, our results show that the morphofunctional differences among locomotor modes are best described as a continuum rather than as discrete features. Moreover, we hypothesize that the pattern of evolutionary transformations from one locomotor mode to another could mirror this continuum rather than consist of random or more distant evolutionary jumps across the morphofunctional space (Carrano 1999). Testing this hypothesis within a phylogenetic comparative framework and with developmental insight is beyond the scope of this paper but is an area for future work.

Ecological Diversification of Mesozoic Mammals

Paleontologists used to view Mesozoic mammals as mostly generalized, small-bodied, nocturnal insectivores (e.g. Lillegraven et al. 1979), seemingly restricted to these limited ecological roles by selection pressures (e.g., predation, competition) imposed by dinosaurs (Van Valen and Sloan 1977; Stucky 1990). This view, however, has begun to fade in the face of recent discoveries of relatively complete mammal fossils (e.g., *Zhangheotherium*, *Yanoconodon*, *Eomaia*) and large-scale quantitative analyses of ecomorphology (Wilson et al. 2012; Wilson 2013; Grossnickle and Polly 2013). In his review of Mesozoic mammal evolution, Luo (2007: Fig. 2) identified five ecomorphs (semiaquatic carnivore/omnivore, terrestrial carnivore/scavenger, fossorial colonial insectivore, scansorial/climbing insectivore, and gliding insectivore/omnivore) present among Mesozoic mammals, in addition to the conventional "terrestrial-generalized insectivore/omnivore/herbivore" category. This more generous view of the ecomorphological diversity of Mesozoic mammals, however, was based on ecomorph assignments from previous studies that variously employed qualitative and quantitative approaches. Subsequently, Wilson et al. (2012) and Grossnickle and Polly (2013) separately documented an expansion in the range of feeding ecomorphs among some mammals (e.g., multituberculates) during the late Mesozoic. In each study, the authors used a robust quantitative approach to a synoptic craniodental data set. However, despite the accumulation of postcranial data in recent years, a similar approach has not been taken to infer the diversity of locomotor modes among Mesozoic mammals. For example, several studies using the phalangeal index (PI) have tested for arboreality vs. scansoriality vs. terrestriality in individual Mesozoic mammals (e.g., Ji et al. 2002; Chen and Luo 2013; Zhou et al. 2013; Zheng et al. 2013), but have quantitatively analyzed few other informative aspects of postcranial morphology. Thus, our study provides the first comprehensive quantitative test of locomotor diversity in Mesozoic mammals, focusing on a phylogenetically broad sample of ten taxa with relatively well-preserved postcranial skeletons. Because locomotor mode has previously been inferred for several of these taxa, our analysis also provides a separate test of those ecomorphological analyses.

From our multivariate analysis of the morphometric data in this modest sample of fossil mammals, we infer the presence of at least five locomotor modes (arboreal, scansorial, semiaquatic, semifossorial, and fossorial) among Mesozoic mammals (Table 1). The Early Cretaceous *Eomaia*, one of the earliest eutherian mammals, was previously inferred as arboreal or scansorial on the basis of the phalangeal index (PI) and comparative anatomical study of its postcranial skeleton (Ji et al. 2002). The ambiguity in this assignment reflects the difficulty in distinguishing arboreal and scansorial modes in extant small-bodied mammals by using osteological features (Jenkins 1974; Schilling and Fischer 1999). Indeed, we also found that in our extensive extant data set the morphological transformation from scansorial to arboreal is gradational with respect to our indices (Fig. 3A,B). For example, in adapting for climbing and branch-working, both arboreal and scansorial mammals have relatively slender limb elements without well-developed tubercles and crests. In our CVAs, the morphological differences between arboreal and scansorial taxa were apparent only in the three-locomotor-mode analysis (Supplementary Fig. 3A). In that analysis, scansorial taxa separate from arboreal taxa on the basis of their more elongate

forelimbs, larger palms, and more elongate phalanges. This characterization does not fit what is observed in *Eomaia*, and, in turn, our analysis predicted that *Eomaia* was arboreal not scansorial (Fig. 6, Supplementary Figs. 4, 5). This assignment is also consistent with other indicators of arboreality (e.g., well-developed scapular acromion and coracoid process [Argot 2001]) that were not captured by our indices but were recognized by Ji et al. (2002) in their study of *Eomaia*.

The Early Cretaceous eutriconodontan *Jeholodens* was previously inferred to be a terrestrial mammal capable of climbing on uneven substrates (Ji et al. 1999). It has a number of plesiomorphic features of the pelvic girdle and hind limb that are primarily associated with terrestrial locomotion in premammalian cynodonts (Ji et al. 1999). However, our multivariate analyses indicate that *Jeholodens* was an arboreal taxon that spent more time in the trees than on the ground (Table 1, Fig. 6, Supplementary Figs. 4, 5). This locomotor inference is consistent with the more derived pectoral girdle and forelimb of *Jeholodens* (Ji et al. 1999). The pectoral girdle has a mobile scapuloclavicular joint and a non-rigid claviculo-interclavicle joint, which together form a mobile and pivotal joint. Its scapula bears a well-demarcated triangular fossa on the dorsoposterior margin that forms a large area of attachment for the teres major muscle (Ji et al. 1999). This muscle functions in the retraction of the forelimb, a motion that is especially important in climbing (Salton and Sargis 2008). In addition to these features, our CVA indicates that the tubercles and processes of the humerus, ulna, and femur (e.g., the lesser and greater tubercles, the olecranon process, and greater trochanter, respectively) are relatively reduced in *Jeholodens*, a condition commonly associated with scansorial and arboreal locomotion. Moreover, *Jeholodens* has a relatively large hand, comparable in size to those of extant small-bodied arboreal and scansorial mammals, implying that the hand was prehensile. Together, these lines of evidence support our interpretation that *Jeholodens* was an arboreal mammal.

The basalmost multituberculate *Rugosodon* from the Middle Jurassic of China was previously inferred as a terrestrial mammal, on the basis of the phalangeal index (PI) and slenderness index (=inverse of our phalangeal robustness index; Yuan et al. 2013). However, as noted by those authors in their supplementary information, the PI of *Rugosodon* plots with terrestrial didelphids, diprodonts, sciuromorph rodents, and euarchontans (Weisbecker and Warton 2006; Kirk et al. 2008) as well as scansorial and arboreal hystricognath rodents and carnivorans (Weisbecker and Schmid 2007; Kirk et al. 2008). In our analyses, the PI of *Rugosodon* is 1.05, which is at the lower limit for arboreal taxa and within the range of our scansorial and terrestrial taxa. Our intermediate phalangeal robustness index (~0.26), which corresponds to the inverse of the intermediate phalangeal slender index of Yuan et al. (2013), places *Rugosodon* in the range of arboreal and scansorial taxa. In light of the subtle morphometric gradation from terrestrial to scansorial to arboreal taxa, it is not surprising that individual osteological indices do not sufficiently distinguish among these locomotor modes. However, using our more comprehensive morphometric scheme in our multivariate analysis, we predict with high posterior probability that *Rugosodon* was a scansorial mammal that was adapted for both climbing and ground walking (Table 1, Fig. 6, Supplementary Figs. 4, 5).

The symmetrodontan *Zhangheotherium quinquecuspidens* was previously inferred as a ground-dwelling mammal on the basis of anatomical observations of the forelimb (Hu et al. 1997, 1998). However, our CVAs classify an unpublished specimen of *Zhangheotherium* (species undetermined) as scansorial. The analyses indicate that *Zhangheotherium* had a relatively large hand with elongate metacarpals and phalanges. The hand proportions are similar to those of extant scansorial taxa, whereas the robustness of the phalanges closely resembles that of extant arboreal taxa. The new specimen of *Zhangheotherium* also has a small olecranon process of the ulna, a feature that is common among both scansorial and arboreal mammals. However, our CVAs indicate that *Zhangheotherium* has other features that differ from those of scansorial mammals. Specifically, extant scansorial taxa tend to have

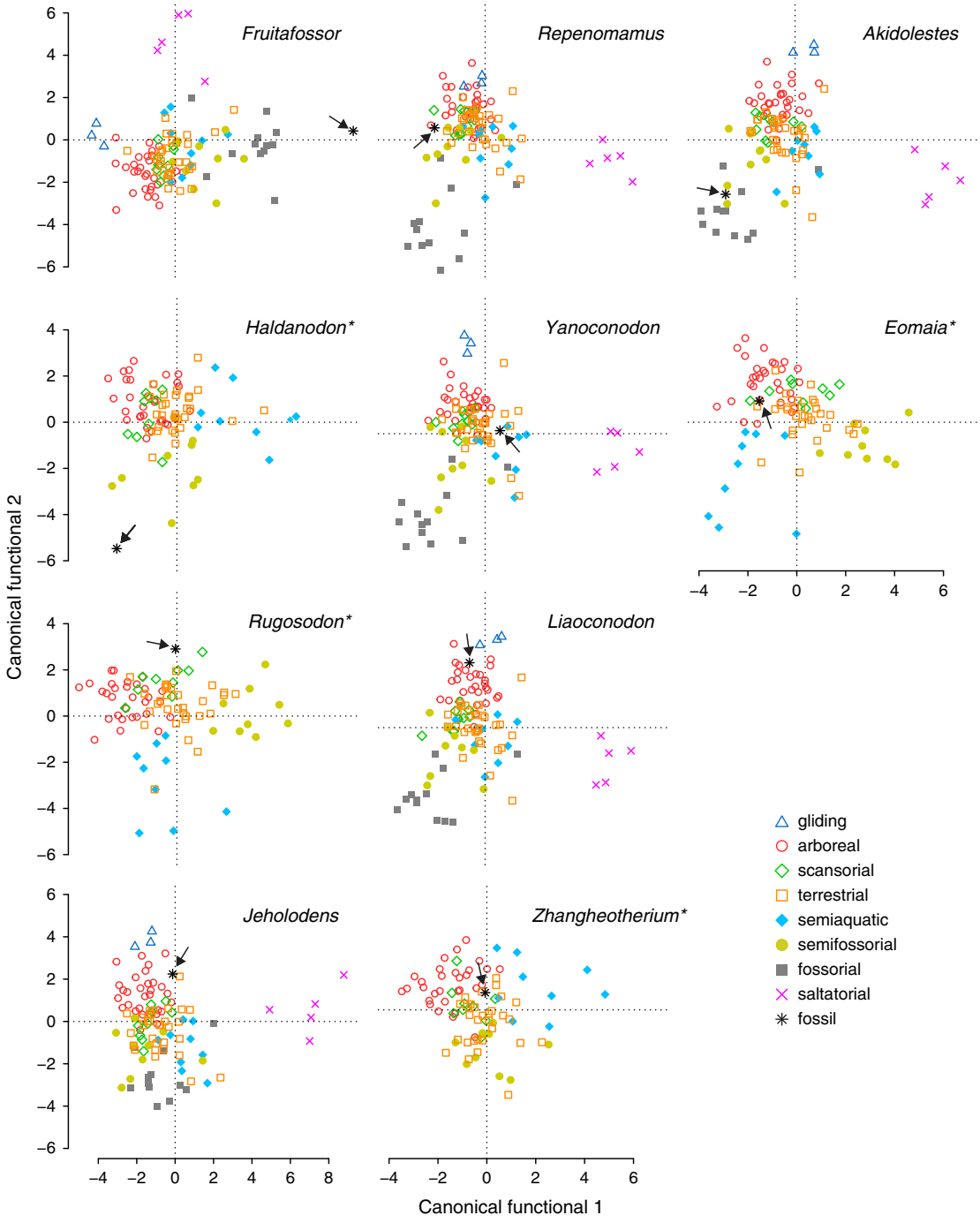

FIGURE 6. Ordinations of ten Mesozoic mammals in the locomotor morphospace. Because each Mesozoic taxon has a unique morphometric data set, each multivariate analysis produced a unique locomotor ordination in the morphospace. Arrows indicate where each fossil taxon plots. An asterisk after the taxon name indicates that the five-locomotor-mode analysis was used for the plot.

elongate forelimbs for ascending and descending trees. In contrast, *Zhangheotherium* has relatively elongate hind limbs, which in extant small-bodied mammals is correlated with hind limb-dominated locomotion, such as hopping or hind-limb-paddle swimming. Moreover, metatarsals II

and III of *Zhangheotherium* are anteroposteriorly elongate and bilaterally expanded, implying that this unpublished specimen of *Zhangheotherium* had a large plantar area of the foot. This region of the foot was missing in the holotype specimen (Hu et al. 1997, 1998). We note, however, that because of poor preservation of the unpublished specimen, we were able to include only 16 osteological indices. Thus, we tentatively follow the locomotor inference of the CVAs to interpret *Zhangheotherium* as a scansorial mammal from the Early Cretaceous (Table 1, Fig. 6, Supplementary Figs. 4, 5).

Full descriptions and functional morphological analyses of the postcranial skeleton of *Yanoconodon* and *Liaoconodon* have not yet been published, but our analyses of the morphometric data indicate that both of these Early Cretaceous eutriconodontans were semiaquatic (Table 1, Fig. 6, Supplementary Figs. 4, 5). Another Mesozoic mammal that was not included in our analysis, the Middle Jurassic docodontan *Castorocauda*, has also been interpreted as semiaquatic (Ji et al. 2006). Despite the shared locomotor assignment, these two eutriconodontans and *Castorocauda* have clear differences in postcranial morphology that indicate different swimming strategies. *Castorocauda* possesses dorsoventrally compressed caudal vertebrae with bifurcated transverse processes that are similar to those of the river otter *Lontra canadensis* and a broad, scaly tail that resembles that of the modern beaver, *Castor canadensis* (Ji et al. 2006); this might imply that, like the modern beaver, *Castorocauda* occasionally used its tail for sculling (Howell 1930). In contrast, *Yanoconodon* and *Liaoconodon* lack those specialized swimming adaptations of the caudal vertebrae, but possess other features of semiaquatic mammals. Their relatively robust limb elements are well suited to resist the stresses incurred during the propulsive swimming stroke. *Yanoconodon* and *Liaoconodon* also have relatively large hands and feet, which presumably facilitated paddling even without webbed fingers. Moreover, the phalanges of the manus of *Yanoconodon* diverge distally, forming a funnel shape, which may be correlated with swimming locomotion. Although we did not analyze indices of the axial skeleton, the elongate trunk of these two eutriconodontans may also be an adaption for swimming, as in the semiaquatic American mink, *Neovison vison*.

Three Mesozoic taxa are inferred as semifossorial: the Late Jurassic docodontan *Haldanodon exspectatus*, the Early Cretaceous eutriconodontan *Repenomamus robustus*, and the Early Cretaceous symmetrodontan *Akidolestes cifellii* (Table 1, Fig. 6; Supplementary Figs. 4, 5). *Akidolestes* was initially inferred as a scansorial mammal by Chen and Luo (2013), on the basis of qualitative comparisons to living arboreal and terrestrial marsupials. In contrast, the interpretation forwarded here, which we argue is more robust because it is based on quantitative multivariate analysis of an extensive data set of extant small-bodied mammals specimens, indicates that *Akidolestes* was a semifossorial mammal. In general, the postcranial skeletons of all three taxa have well-developed tubercles and crests of the forelimbs and hind limbs for attachment of relatively large muscles as in extant digging mammals. The diaphyses of their limb elements are more slender than those of fossorial taxa, as reflected by their robustness index values, which are closer to those of extant semifossorial taxa than those of fossorial taxa. Nevertheless, the postcranial morphologies of these three semifossorial fossil mammals differ from one another. As a stem mammal, the docodontan *Haldanodon* retains some plesiomorphic postcranial features that are shared with, for example, premammalian cynodonts, morganucodontans, and monotremes (Kühne 1956; Klima 1973; Sun and Li 1985; Jenkins and Parrington 1976; Martin 2005; Sues and Jenkins 2006), but are lost in more nested mammalian taxa, like *Repenomamus* and *Akidolestes*. For example, *Haldanodon* has an hourglass-shaped humerus that bears a broad proximal head and a well-developed deltopectoral crest, which is similar to that of the short-beaked echidna, *Tachyglossus aculeatus* (Martin 2005). In contrast, the humerus of *Akidolestes* is relatively longer and less robust than that of *Haldanodon*. Its distal end bears a trochlear articular facet for the ulna (Chen and Luo 2013), as in living therians but absent in *Haldanodon*. Furthermore, the degree of torsion along the humeral diaphysis differs between *Haldanodon* (60°) and *Akidolestes* (40°),

corresponding, respectively, to a more sprawling posture vs. a more parasagittal one. In general, the postcranial elements of *Repenomamus* (Hu 2006) show an intermediate stage of development between the less robust postcranial elements of *Akidolestes* and the more robust postcranial elements of *Haldanodon*. In other aspects, *Repenomamus* strongly differs from *Haldanodon* and *Akidolestes*. The scapula of *Repenomamus* has curved anterior and dorsal margins, whereas *Haldanodon* and *Akidolestes* have scapulae with straight margins. This degree of morphological variance among semifossorial Mesozoic mammals parallels the large morphological variance in our sample of semifossorial extant taxa, and likewise probably stems from a combination of phylogenetic diversity and functional diversity.

The Late Jurassic *Fruitafossor windscheffeli* has uncertain phylogenetic affinities among stem mammals, but its locomotor mode is unequivocally fossorial, as inferred by our analysis and the analysis of Luo and Wible (2005) (Table 1, Fig. 6; Supplementary Fig. 4). *Fruitafossor* possesses a number of adaptations for digging, including a bilaterally expanded humerus with well-developed tubercles and crests forming a large area for muscle attachment, an enlarged olecranon process of the ulna that increases the size of the input lever, hypertrophied manual elements for efficiently removing soil, and elongate distal phalanges for effectively loosening soil (Hildebrand 1985; Stein 2000; Hopkins and Davis 2009). Luo and Wible (2005) further suggested that the dental and vertebral anatomy of *Fruitafossor* is convergent with that of extant xenarthran diggers that use a scratch digging sub-mode (Hildebrand 1985). *Fruitafossor* is similar in many shoulder girdle and limb features to *Tachyglossus*, which has been known to use scratch digging and hook-and-pull digging (Augee et al. 2006). Additionally, we note that the scapula and forelimb of *Fruitafossor* are comparable to moles that are humeral-rotation diggers (*sensu* Hildebrand 1985; Hildebrand and Goslow 1998), such as the extant mole *Scapanus*.

Taken together, our locomotor inferences of these ten Mesozoic taxa and those from previous studies of 19 other taxa begin to paint a more complete picture of the temporal and phylogenetic pattern of locomotor diversification among Mesozoic mammals (Fig. 7). The Late Triassic record of mammalian postcranial skeletons is limited to a single taxon, the stem mammal *Morganucodon*, which has been interpreted as a generalized terrestrial mammal (Jenkins and Parrington 1976). By the late Middle Jurassic, we see substantial locomotor diversification: the gliding ?eutricondontan *Volaticotherium* (Meng et al. 2006), the arboreal haramiyidan *Arboroharamiya* (Zheng et al. 2013), the terrestrial haramiyidan *Megaconus* (Zhou et al. 2013), and the semiaquatic docodontan *Castorocauda* (Ji et al. 2006). The Late Jurassic may represent a peak in locomotor diversification, in which the docodontan *Haldanodon*, the stem mammal *Fruitafossor*, the multituberculate *Rugosodon*, and the basal cladotherian *Henkelotherium* (Krebs 1991; Vázquez-Molinero et al. 2001; Jäger et al. 2013) further expand the range of locomotor modes to include semifossorial, fossorial, scansorial, and arboreal, respectively.

Then, in the Early Cretaceous, there are examples of repeated, independent evolution of these six locomotor modes in different lineages (Fig. 7). The eutriconodontans *Yanoconodon* and *Liaoconodon*, like the Middle Jurassic *Castorocauda*, were semiaquatic forms, although they may have differed from *Castorocauda* in swimming strategy. Moreover, the eutriconodontan *Jeholodens* (arboreal), the multituberculate *Sinobaatar* (arboreal [Hu and Wang 2002]), the symmetrodontan *Zhangheotherium* (scansorial), the eutherian *Eomaia* (arboreal), and the metatherian *Sinodelphys* (scansorial/arboreal) show climbing adaptations like Late Jurassic *Arboroharamiya* and *Henkelotherium*; the eutriconodontan *Gobiconodon ostromi* shows ground-dwelling adaptations (terrestrial); and the symmetrodontan *Akidolestes* and the eutriconodontan *Repenomamus* show burrowing adaptations (semifossorial), although they may have had sub-modes distinct from each other and from the Late Jurassic *Haldanodon*. In the Late Cretaceous, the range of locomotor modes further expanded to include the saltatorial mode. The multituberculates *Catopsbaatar*, *Kryptobaatar*, and *Nemegtbaatar* (Kielan-Jaworowska and Gambaryan 1994; Hurum and Kielan-Jaworowska 2008) and the

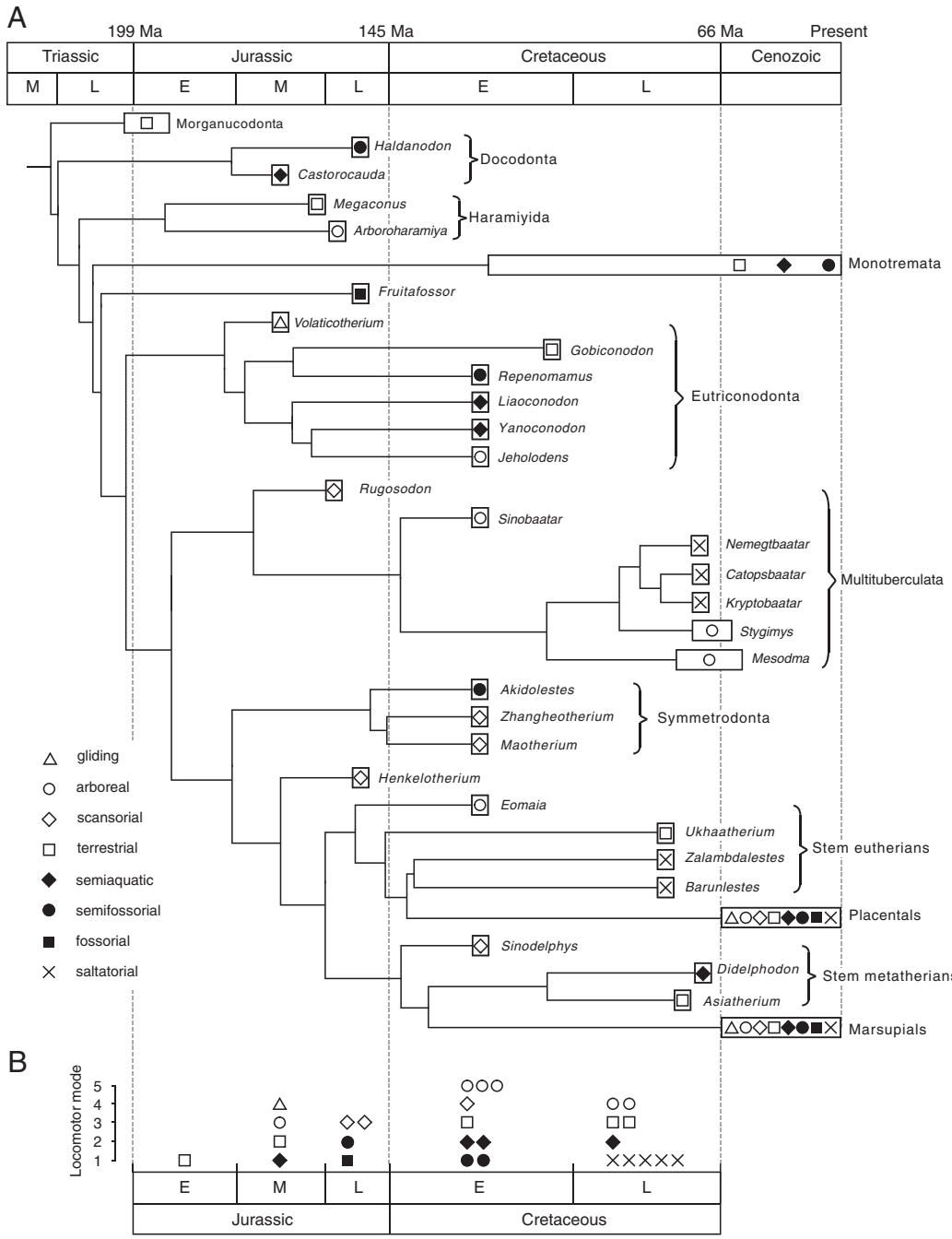

FIGURE 7. Locomotor diversification of mammals from the Early Jurassic to the present. A, Distribution of locomotor modes across the phylogeny of Mesozoic mammals (phylogeny is based on Kielan-Jaworowska and Hurum 2001, Luo 2007, Yuan et al. 2013, Zheng et al. 2013, and Zhou et al. 2013). We followed the placement of Haramiyida in Zhou et al. 2013 (but see Zheng et al. 2013 for a different placement). Stratigraphic ranges of taxa (rectangles bounding symbols) are based on Kielan-Jaworowska et al. (2004) and the primary literature. We mapped the inferred locomotor mode of 29 Mesozoic taxa that have relatively well-preserved postcranial skeletons, of which ten were analyzed in this study (see Table 1). The locomotor inferences of the other 19 taxa are based on previous functional morphological studies (see text). B, Distribution of locomotor modes through time, from the Early Jurassic to the Late Cretaceous. Symbols indicate which locomotor modes were present in each time interval and the number of taxa from that locomotor mode.

eutherians *Zalambdalestes* and *Barunlestes*, all from Asia, have been interpreted as saltatorial and/or terrestrial runners (Kielan-Jaworowska 1978; Chester et al. 2010, 2012). In contrast, the Late Cretaceous and Paleogene multituberculates *Mesodma* and *Stygimys* from North America may have employed an arboreal mode (Krause and Jenkins 1983), whereas the eutherian *Ukhaatherium* (Horovitz 2003; Kielan-Jaworowska et al. 2004) and the metatherian *Asiatherium* (Kielan-Jaworowska et al. 2004), both from Asia, have been interpreted as terrestrial, and the Late Cretaceous metatherian *Didelphodon* has been interpreted as possibly semiaquatic on the basis of isolated elements that can only be tentatively associated (Szalay 1994; Longrich 2004; but see Fox and Naylor 2006 and Borths and Hunter 2008).

This pattern of locomotor diversification among Mesozoic mammals also differed across clades (Fig. 7). The Multituberculata, arguably the most successful clade of Mesozoic mammals (Wilson et al. 2012), has a relatively small sample of postcranial fossils that have led to sometimes-divergent interpretations of locomotor modes among Mesozoic multituberculates (e.g., Gambaryan and Kielan-Jaworowska 1997; Sereno 2006). Accordingly, multituberculates may have diversified into arboreal, scansorial, terrestrial, as well as saltatorial forms during the Mesozoic (Krause and Jenkins 1983; Kielan-Jaworowska and Gambaryan 1994; Hu and Wang 2002; Sereno 2006; Yuan et al. 2013). Another highly successful clade, the Eutriconodonta, had representatives of at least four locomotor modes: arboreal (this study), terrestrial (Jenkins and Schaff 1988), semiaquatic (this study), and semifossorial modes (Hu 2006; this study); and if assignment of *Volaticotherium* to the Eutriconodonta is upheld (Gaetano and Rougier 2011, 2012), it would add a gliding form to this clade. As such, eutriconodontans may have achieved the greatest locomotor diversity of any mammal clade up until the Early Cretaceous. In contrast, only four locomotor modes have been inferred for the Metatheria (arboreal, scansorial, terrestrial, and possibly semiaquatic [Szalay 1994; Luo et al. 2002; Horovitz 2003; Kielan-Jaworowska et al. 2004; Longrich 2004; Chester et al. 2010, 2012]), and only two for the Docodonta (semiaquatic and semifossorial [Ji et al. 2006; this study]), "Symmetrodonta" (semifossorial and terrestrial [Hu et al. 1997, 1998; Luo and Ji 2005; this study]), and Eutheria (arboreal and saltatorial [Kielan-Jaworowska 1978; this study]). In sum, Mesozoic mammals did achieve greater locomotor diversity than is generally appreciated, as hypothesized by Luo (2007), but it seems that this diversification was not fully under way until the Late Jurassic and even then it did not include all clades. We emphasize, however, that our picture of locomotor diversification among Mesozoic mammals should be viewed as a conservative estimate. With the pace of discovery of relatively complete Mesozoic mammal skeletons showing no signs of slowing down, we expect that in the not too distant future many of the temporal and phylogenetic gaps presented here could be filled in.

Conclusions

In this paper, our multivariate analyses of a large postcranial morphometric data set show that extant small-bodied mammals of different locomotor modes have subtle but detectable and functionally relevant morphological differences. Ordination of these locomotor modes via linear canonical variate analysis illustrates what we term a morphofunctional continuum; that is, a gradient of locomotor modes reflecting their biomechanical requirements and adaptations under natural selection. We speculate that the pattern of evolutionary transformations from one locomotor mode to another, at least in small-bodied mammals, may be best explained in the context of this morphofunctional continuum, as well as external selective pressures that these small-bodied mammals faced in the Mesozoic (e.g., vegetational structure, predation, competition [Wing and Tiffney 1987]). We applied our more comprehensive, multivariate approach to locomotor inference to postcranial skeletons of ten Mesozoic mammal taxa. In some cases, our results confirmed previous locomotor inferences, and in other cases differed from them. Viewing these interpretations along with other robust studies serves to further shift the paradigm away from the notion that the Mesozoic represented the "dark ages" for mammalian evolution (Luo 2007). Instead, it

appears that by the Late Jurassic mammals had diversified into seven of the eight locomotor modes that we recognized in this study. The degree of locomotor diversification varied across Mesozoic mammal clades, but seems to have been most pronounced in the Eutriconodonta and the Multituberculata, although sampling of postcranial skeletons is still a major issue.

Acknowledgments

We would like to thank D. Lunde (Smithsonian Institute National Museum of Natural History), E. Westwig (American Museum of Natural History), W. Stanley and R. Banasiak (Field Museum of Natural History), and J. Bradley (University of Washington Burke Museum of Natural History and Culture) for access to and assistance with the mammal collections at their respective institutions. We are indebted to Z.-X. Luo (University of Chicago); Q.-J. Meng, Z.-H. Zeng, L.-D. Liu, and D. Liu (Beijing Museum of Natural History); Q. Ji and Q.-X. Yuan (Chinese Academy of Geological Science); C.-L Gao (Dalian Museum of Natural History); P.-J. Chen and G. Li (Nanjing Institute of Geology and Paleontology); and X.-N. Yang, Y.-K. Shi, and B.-Y. Jiang (Nanjing University) for providing access to some of the Mesozoic fossil specimens included in this study. We are grateful for valuable suggestions and discussions offered by Z.-X. Luo, D. Polly, J. Samuels, and C. Sidor. We also thank members of the Wilson Lab (J. Calede, L. DeBey, D. DeMar Jr., and S. Smith) for useful comments on earlier drafts of this manuscript. We thank three reviewers, S. Chester, T. Martin, and Z.-X. Luo, for their comments and suggestions and helping us improve this manuscript. We gratefully acknowledge funding for this project to M.C by the Washington Research Foundation-Hall Fellowship and to G.W. and M.C. from the University of Washington Department of Biology.

Literature Cited

Alexander, R. M. 1985. Body support, scaling, and allometry. Pp. 26–37 *In* Hildebrand et al. 1985.

Alexander, R. M, A. S. Jayes, G. M. Maloiy, and E. M. Wathuta. 1981. Allometry of the leg muscles of mammals. Journal of Zoology 194:539–552.

Allin, E.F., and J. A. Hopson. 1992. Evolution of the auditory system in Synapsida ("mammal-like reptiles" and primitive mammals) as seen in the fossil record. Pp. 587–614 *In* D. B. Webster, R. R. Fay, and A. N. Popper, eds. The evolutionary biology of hearing. Springer, New York.

Argot, C. 2001. Functional-adaptive anatomy of the forelimb in the Didelphidae, and the paleobiology of the Paleocene marsupials *Mayulestes ferox* and *Pucadelphys andinus*. Journal of Morphology 247:51–79.

——. 2002. Functional-adaptive analysis of the hindlimb anatomy of extant marsupials and the paleobiology of the Paleocene marsupials *Mayulestes ferox* and *Pucadelphys andinus*. Journal of Morphology 253:76–108.

Augee, M., B. Gooden, and A. Musser. 2006. Echidna: extraordinary egg-laying mammal. CSIRO Publishing, Collingwood, Australia.

Bassarova, M., C. M. Janis, and M. Archer. 2009. The calcaneum—on the heels of marsupial locomotion. Journal of Mammalian Evolution 16:1–23.

Beard, K. C. 1993. Origin and evolution of gliding in Early Cenozoic Dermoptera (Mammalia, Primatomorpha). Pp. 63–90 *In* R. D. E. MacPhee, ed. Primates and their relatives in phylogenetic perspective. Plenum, New York.

Biewener, A. A. 1989. Mammalian terrestrial locomotion and size. Bioscience 39:776–783.

——. 1990. Biomechanics of mammalian terrestrial locomotion. Science 250:1097.

——. 2003. Animal locomotion. Oxford University Press, Oxford.

Bloch, J. I., and D. M. Boyer. 2002. Grasping primate origins. Science 298:1606–1610.

Boyer, D. M., G. S. Yapuncich, S. G. B. Chester, J. I. Bloch, and M. Godinot. 2013. Hands of early primates. Yearbook of Physical Anthropology 57:33–78.

Borths, M., and J. P. Hunter. 2008. Gimme shelter? Locomotor trends and mammalian survivorship at the K/Pg boundary. Journal of Vertebrate Paleontology 28:54–55A.

Bourlière, F. 1975. Mammals, small and large: the ecological implications of size. Pp. 1–8 *in* F. B. Golley, K. Petrusewicz, and L. Ryszkowski, eds. Small mammals: their productivity and population dynamics. Cambridge University Press, Cambridge.

Bover, P., J. A. Alcover, J. J. Michaux, L. Hautier, and R. Hutterer. 2010. Body shape and life style of the extinct Balearic dormouse *Hypnomys* (Rodentia, Gliridae): new evidence from the study of associated skeletons. PLoS ONE 5(12):e15817. doi:10.1371/journal.pone.0015817.

Carrano, M. T. 1999. What, if anything, is cursor? Categories versus continua for determining locomotor habit in mammals and dinosaurs. Journal of Zoology 247:29–42.

Cartmill, M. 1985. Climbing. Pp. 73–88 *In* Hildebrand et al. 1985.

Chen, M., and Z.-X. Luo. 2013. Postcranial skeleton of the Cretaceous mammal *Akidolestes cifellii* and its locomotor adaptations. Journal of Mammalian Evolution 20:159–189.

Chester, S. G. B., E. J. Sargis, F. S. Szalay, J. D. Archibald, and A. O. Averianov. 2010. Mammalian distal humeri from the Late Cretaceous of Uzbekistan. Acta Palaeontologica Polonica 55:199–211.

Chester, S. G. B., E. J. Sargis, F. S. Szalay, J. D. Archibald, and A. O. Averianov. 2012. Therian femora from the Late Cretaceous of Uzbekistan. Acta Palaeontologica Polonica 57:53–64.

Croft, D. A., and L. C. Anderson. 2008. Locomotion in the extinct notoungulate *Protypotherium*. Palaeontologia Electronica 11: 1–20.

Degen, A. A. 1997. Ecophysiology of small desert mammals. Springer, Berlin.

Dunstone, N. 1979. Swimming and diving behavior of the mink (*Mustela vison* Schreber). Carnivore 2:56–61.

Elissamburu, A., and S. F. Vizcaíno. 2004. Limb proportions and adaptations in caviomorph rodents (Rodentia: Caviomorpha). Journal of Zoology 262:145–159.

Emerson, S. B. 1985. Jumping and leaping. Pp. 58–72 *in* Hildebrand et al. 1985.

Evans, A. R. 2013. Shape descriptors as ecometrics in dental ecology. Hystrix, Italian Journal of Mammalogy 24:133–140.

Fish, F. E. 1993. Influence of hydrodynamic design and propulsive mode on mammalian swimming energetics. Australian Journal of Zoology 42:79–101.

Fox, R. C., and B. G. Naylor. 2006. Stagodontid marsupials from the Late Cretaceous of Canada and their systematic and functional implications. Acta Palaeontologica Polonica 51: 13–36.

Fröbisch, J., and R. R. Reisz. 2009. The Late Permian herbivore *Suminia* and the early evolution of arboreality in terrestrial vertebrate ecosystems. Proceedings of Royal Society of London B 276:3611–3618.

Gaetano, L. C., and G. W. Rougier. 2011. New materials of *Argentoconodon fariasorum* (Mammaliaformes, Triconodontidae) from the Jurassic of Argentina and its bearing on triconodont phylogeny. Journal of Vertebrate Paleontology 31:829–843.

——. 2012. First amphilestid from South America: a molariform from the Jurassic Cañadón Asfalto Formation, Patagonia, Argentina. Journal of Mammalian Evolution 19:235–248.

Gambaryan, P. P. 1974. How mammals run: anatomical adaptations. Wiley, New York.

Gambaryan, P. P., and Z. Kielan-Jaworowska. 1997. Sprawling versus parasagittal stance in multituberculate mammals. Acta Palaeontologica Polonica 42:13–44.

Gingerich, P. D. 2003. Land-to-sea transition in early whales: evolution of Eocene Archaeoceti (Cetacea) in relation to skeletal proportions and locomotion of living semiaquatic mammals. Paleobiology 29:429–454.

Grillner, S., and P. Wallén. 1985. The ionic mechanisms underlying N-methyl-D-aspartate receptor-induced, tetrodotoxin-resistant membrane potential oscillations in lamprey neurons active during locomotion. Neuroscience Letter 60:289–294.

Grossnickle, D. M., and P. D. Polly. 2013. Mammal disparity decreases during the Cretaceous angiosperm radiation. Proceedings of the Royal Society of London B 280:20132110. doi: 10.1098/rspb.2013.2110.

Hildebrand, M. 1985. Digging in quadrupeds. Pp. 89–109 *in* Hildebrand et al. 1985.

Hildebrand, M., and G. Goslow. 1998. Analysis of vertebrate structure. Wiley, New York.

Hildebrand, M., D. M. Bramble, K. F. Liem, and D. B. Wake, eds. 1985. Functional vertebrate morphology. Harvard University Press, Cambridge.

Hopkins, S. S. B., and E. B. Davis. 2009. Quantitative morphological proxies for fossoriality in small mammals. Journal of Mammalogy 90:1449–1460.

Horovitz, I. 2003. Postcranial skeleton of *Ukhaatherium nessovi* (Eutheria, Mammalia) from the Late Cretaceous of Mongolia. Journal of Vertebrate Paleontology 23:857–868.

Howell, A. B. 1930. Aquatic mammals. Charles C. Thomas, Springfield, Ill.

Hu, Y.-M. 2006. Postcranial morphology of *Repenomamus* (Eutriconodonta, Mammalia): implications for the higher-level phylogeny of mammals. Ph.D. dissertation. City University of New York, New York.

Hu, Y.-M., and Y.-Q. Wang. 2002. *Sinobaatar* gen. nov.: first multituberculate from the Jehol Biota of Liaoning, northeast China. Chinese Science Bulletin 47:933–938.

Hu, Y.-M., Y.-Q. Wang, Z.-X. Luo, and C.-K. Li. 1997. A new symmetrodont mammal from China and its implications for mammalian evolution. Nature 390:137–142.

Hu, Y.-M., Y.-Q. Wang, C.-K. Li, and Z.-X. Luo. 1998. Morphology of dentition and forelimb of *Zhangheotherium*. Vertebrata PalAsiatica 36:102–125.

Hu, Y.-M., J. Meng, Y.-Q. Wang, and C.-K. Li. 2005. Large Mesozoic mammals fed on young dinosaurs. Nature 433:149–152.

Hurum, J. H., and Z. Kielan-Jaworowska. 2008. Postcranial skeleton of a Cretaceous multituberculate mammal *Catopsbaatar*. Acta Palaeontologica Polonica 53:545–566.

Iwaniuk, A. N., S. M. Pellis, and I. Q. Whishaw. 1999. The relationship between forelimb morphology and behaviour in North American carnivores (Carnivora). Canadian Journal of Zoology 77:1064–1074.

Janis, C. M., J. M. Theodor, and B. Boisvert. 2002. Locomotor evolution in camels revisited: a quantitative analysis of pedal anatomy and the acquisition of the pacing gait. Journal of Vertebrate Paleontology 22:110–121.

Jäger, K., Z.-X. Luo, and T. Martin. 2013. CT scanning and 3D image analysis of the postcranial skeleton of *Henkelotherium guimarotae* (Cladotheria, Mammalia) from the Late Jurassic of Portugal and its locomotor adaptations. Society of Vertebrate Paleontology 73rd, Program and Abstracts, p. 147. Journal of Vertebrate Paleontology (online supplement), October 2013.

Jenkins, F. A. 1970. Limb movements in a monotreme (*Tachyglossus aculeatus*): a cineradiographic analysis. Science 168:1473–1475.

——. 1974. Tree shrew locomotion and arborealism. Pp. 85–115 *in* F. A. Jenkins, ed. Primate locomotion. Academy Press, New York.

Jenkins, F. A., and F. Parrington. 1976. Postcranial skeletons of Triassic mammals *Eozostrodon*, *Megazostrodon* and *Erythrotherium*. Philosophical Transactions of the Royal Society of London B 273:387–431.

Jenkins, F. A., and C. R. Schaff. 1988. The Early Cretaceous mammal *Gobiconodon* (Mammalia, Triconodonta) from the Cloverly Formation in Montana. Journal of Vertebrate Paleontology 8:1–24.

Jerison, H. J. 1973. Evolution of the brain and intelligence. Academic Press, New York.

Ji, Q., Z.-X. Luo, and S.-A. Ji. 1999. A Chinese triconodont mammal and mosaic evolution of the mammalian skeleton. Nature 398:326–330.

Ji, Q., Z.-X. Luo, C.-X. Yuan, J. R. Wible, J.-P. Zhang, and J. A. Georgi. 2002. The earliest known eutherian mammal. Nature 416:816–822.

Ji, Q., Z.-X. Luo, C.-X. Yuan, and A. R. Tabrum. 2006. A swimming mammaliaform from the Middle Jurassic and ecomorphological diversification of early mammals. Science 311:1123–1127.

Jouffroy, F. K., and J. Lessertisseur. 1979. Relationships between limb morphology and locomotor adaptations among prosimians: an osteometric study. Pp. 143–181 *In* M. E. Morbeck, H. Preuschoft, and N. Gomberg, eds. Environment, behavior, and morphology: dynamic interactions in primates. Gustav Fischer, New York.

Jouffroy, F. K., M. Godinot, and Y. Nakano. 1993. Biometrical characteristics of primate hands. Pp. 133–171 *In* H. Preuschoft and D. J. Chivers, eds. Hands of primates. Springer, New York.

Kardong, K. V. 2009. Vertebrates: comparative anatomy, function, evolution. McGraw-Hill, New York.

Kelt, D. A., and M. D. Meyer. 2009. Body size frequency distributions in African mammals are bimodal at all spatial scales. Global Ecology and Biogeography 18:19–29.

Kielan-Jaworowska, Z. 1978. Evolution of the therian mammals in the Late Cretaceous of Asia. Part III. Postcranial skeleton in Zalambdalestidae. Acta Palaeontologia Polonica 38:5–41.

Kielan-Jaworowska, Z., and P. P. Gambaryan. 1994. Postcranial anatomy and habits of Asian multituberculate mammals. Fossil and Strata 36:1–92.

Kielan-Jaworowska, Z., R. L. Cifelli, and Z.-X. Luo. 2004. Mammals from the age of dinosaurs: origins, evolution, and structure. Columbia University Press, New York.

Kingdon, J. 1997. The Kingdon field guide to African mammals. Academic Press, San Diego.

Kirk, E. C., P. Lemelin, M. W. Hamrick, D. M. Boyer, and J. I. Bloch. 2008. Intrinsic hand proportions of euarchontans and other mammals: implications for the locomotor behavior of plesiadapiforms. Journal of Human Evolution 55:278–299.

Klima, M. 1973. Die Frühentwicklung des Schultergürtels und des Brustbeins bei den Monotremen (Mammalia: Prototheria). Advances in Anatomy, Embryology and Cell Biology 47:1–80.

Krause, D. W., and F. A. Jenkins. 1983. The postcranial skeleton of North American multituberculates. Bulletin of the Museum of Comparative Zoology 150:199–246.

Krebs, B. 1991. Das Skelett von *Henkelotherium guimarotae* gen. et sp. nov. (Eupantotheria, Mammalia) aus dem Oberen Jura yon Portugal. Berliner Geowissenschaftliche Abhandlungen A 133: 1–121.

Kühne, W. G. 1956. The Liassic therapsid *Oligokyphus*. British Museum (Natural History), London.

Lanyon, L. E., and C. T. Rubin. 1985. Functional adaptation in skeletal structures. Pp. 1–25 *In* Hildebrand et al. 1985.

Lemelin, P. 1999. Morphological correlates of substrate use in didelphid marsupials: implications for primate origins. Journal of Zoology 247:165–175.

Li, G., and Z.-X. Luo. 2006. A Cretaceous symmetrodont therian with some monotreme-like postcranial features. Nature 439: 195–200.

Lillegraven, J. A., Z. Kielan-Jaworowska, and W. A. Clemens. 1979. Mesozoic mammals: the first two-thirds of mammalian history. University of California Press, Berkeley.

Longrich, N. 2004. Aquatic specialization in mammals from the Late Cretaceous of North America. Journal of Vertebrate Paleontology 24(Suppl. to No. 3): 84A.

Luo, Z.-X. 2007. Transformation and diversification in early mammal evolution. Nature 450:1011–1019.

Luo, Z.-X., and Q. Ji. 2005. New study on dental and skeletal features of the Cretaceous "symmetrodontan" mammal *Zhangheotherium*. Journal of Mammalian Evolution 12:337–357.

Luo, Z.-X., and J. R. Wible. 2005. A Late Jurassic digging mammal and early mammalian diversification. Science 308: 103–107.

Luo, Z.-X., R. L. Cifelli, and Z. Kielan-Jaworowska. 2001a. Dual origin of tribosphenic mammals. Nature 409:53–57.

Luo, Z.-X., A. W. Crompton, and A.-L. Sun. 2001b. A new mammaliaform from the early Jurassic and evolution of mammalian characteristics. Science 292:1535–1540.

Luo, Z.-X., Q. Ji, J. R. Wible, and C.-X. Yuan. 2003. An Early Cretaceous tribosphenic mammal and metatherian evolution. Science 302:1934–1940.

Luo, Z.-X., P.-J. Chen, G. Li, and M. Chen. 2007. A new eutriconodont mammal and evolutionary development in early mammals. Nature 446:288–293.

MacLeod, N., and K. D. Rose. 1993. Inferring locomotor behavior in Paleogene mammals via eigenshape analysis. American Journal of Science 293A:300–355.

Martin, T. 2005. Postcranial anatomy of *Haldanodon exspectatus* (Mammalia, Docodonta) from the Late Jurassic (Kimmeridgian) of Portugal and its bearing for mammalian evolution. Zoological Journal of the Linnean Society 145:219–248.

——. 2013. Mammalian postcranial bones from the Late Jurassic of Portugal and their implications for forelimb evolution. Journal of Vertebrate Paleontology 33:1432–1441.

Marshall, L. G. 1978. *Chironectes minimus*. Mammalian Species 109:1–6.

McMahon, T. A. 1975. Using body size to understand the structural design of animals: quadrupedal locomotion. Journal of Applied Physiology 39:619–627.

McNab, B. K. 1990. Physiological significance of body size. Pp. 11–24 *In* J. D. Damuth and B. J. MacFadden, eds. Body size in mammalian paleobiology: estimation and biological implications. Cambridge University Press, Cambridge.

——. 2002. The physiological ecology of vertebrates: a view from energetics. Cornell University Press, New York.

Meng, J., Y.-M. Hu, Y.-Q. Wang, X.-L. Wang, and C.-K. Li. 2006. A Mesozoic gliding mammal from northeastern China. Nature 444:889–893.

Merritt, J. F. 2010. The biology of small mammals. Johns Hopkins University Press, Baltimore.

Nakagawa, M., H. Miguchi, K. Sato, S. Shoko, and T. Nakashizuka. 2007. Population dynamics of arboreal and terrestrial small mammals in a tropical rainforest, Sarawak, Malaysia. Raffles Bulletin of Zoology 55:389–395.

Nowak, R. M. 1999. Walker's mammals of the world. Johns Hopkins University Press, Baltimore.

——. 2005. Walker's marsupials of the world. Johns Hopkins University Press, Baltimore.

O'Keefe, F. R, and M. T. Carrano. 2005. Correlated trends in the evolution of the plesiosaur locomotor system. Paleobiology 31:656–675.

Polly, P. D. 2007. Limbs in mammalian evolution. Pp. 245–268 *In* B. K. Hall, ed. Fins into limbs: evolution, development and transformation. University of Chicago Press, Chicago.

——. 2008. Adaptive zones and the pinniped ankle: a three-dimensional quantitative analysis of carnivoran tarsal evolution. Pp. 167–196 *In* E. J. Sargis and M. Dagosto, eds. Mammalian evolutionary morphology. Springer, Dordrecht.

——. 2011. Tiptoeing through the trophics: geographic variation in carnivoran locomotor ecomorphology in relation to environment. Pp. 374–410 *In* A. Goswami and A. R. Friscia, eds. Carnivoran evolution: new views on phylogeny, form and function. Cambridge University Press, Cambridge.

Rowe, T. B. 1996. Coevolution of the mammalian middle ear and neocortex. Science 273:651–654.

Rowe, T. B., T. E. Macrini, and Z. X. Luo. 2011. Fossil evidence on origin of the mammalian brain. Science 332:955–957.

Salton, J. A. and E. J. Sargis. 2008. Evolutionary morphology of the Tenrecoidea (Mammalia) forelimb skeleton. Pp. 51–77 *In* E. J. Sargis and M. Dagosto, eds. Mammalian evolutionary morphology. Springer, Dordrecht.

Samuels, J. X., and B. Van Valkenburgh. 2008. Skeletal indicators of locomotor adaptations in living and extinct rodents. Journal of Morphology 269:1387–1411.

Samuels, J. X., J. A. Meachen, and S. A. Sakai. 2013. Postcranial morphology and the locomotor habits of living and extinct carnivorans. Journal of Morphology 274:121–146.

Sargis, E. J. 2001a. The grasping behaviour, locomotion and substrate use of the tree shrews *Tupaia minor* and *T. tana* (Mammalia, Scandentia). Journal of Zoology 253:485–490.

——. 2001b. A preliminary qualitative analysis on the axial skeleton of tupaiids (Mammalia, Scandentia): functional morphology and phylogenetic implications. Journal of Zoology, London 253:473–483.

——. 2002a. Functional morphology of the forelimb of tupaiids (Mammalia. Scandentia) and its phylogenetic implications. Journal of Morphology 253:10–42.

——. 2002b. Functional morphology of the hindlimb of tupaiids (Mammalia. Scandentia) and its phylogenetic implications. Journal of Morphology 254:149–185.

Schilling, N., and M. S. Fischer. 1999. Kinematic analysis of treadmill locomotion of tree shrews, *Tupaia glis* (Scandentia: Tupaiidae). Zeitschrift für Säugetierkunde (International Journal of Mammalian Biology) 64:1–25.

Sereno, P. 2006. Shoulder girdle and forelimb in multituberculates: evolution of parasagittal forelimb posture in mammals. Pp. 315–366 *In* M. T. Carrano, T. J. Gaudin, R. W. Blob, and J. R. Wible, eds. Amniote paleobiology: perspectives on the evolution of mammals, birds, and reptiles. University of Chicago Press, Chicago.

Shattuck, M. R., and S. A. Williams. 2010. Arboreality has allowed for the evolution of increased longevity in mammals. Proceedings of the National Academy of Sciences USA 107:4635–4639.

Shimer, H. W. 1903. Adaptations to aquatic, arboreal, fossorial, and cursorial habits in mammals. III. Fossorial adaptations. American Naturalist 37:819–825.

Sokal, R. R., and F. J. Rohlf. 2012. Biometry: the principles and practice of statistics in biological research, 4th ed. W. H. Freeman, New York.

Stein, B. R. 1988. Morphology and allometry in several genera of semiaquatic rodents (*Ondatra*, *Nectomys*, and *Oryzomys*). Journal of Mammalogy 69:500–511.

——. 2000. Morphology of subterranean rodents. Pp. 19–61 *In* E. A. Lacey, J. L. Patton, and G. N. Cameron, eds. Life underground: the biology of subterranean rodents. University of Chicago Press, Chicago.

Stoddart, D. M. 1979. Ecology of small mammals. Chapman and Hall, London.

Stucky, R. K. 1990. Evolution of land mammal diversity in North America during the Cenozoic. Current Mammalogy 2:375–432.

Sues, H.-D., and F. A. Jenkins. 2006. The postcranial skeleton of *Kayentatherium wellesi* from the Lower Jurassic Kayenta Formation of Arizona and the phylogenetic significance of postcranial features. Pp. 114–152 *In* M. T. Carrano, T. J. Gaudin, R. W. Blob, and J. R. Wible, eds. Amniote paleobiology: perspectives on the evolution of mammals, birds, and reptiles. University of Chicago Press, Chicago.

Sun, A., and Y. Li. 1985. The postcranial skeleton of the late tritylodont Bienotheroides. Vertebrata PalAsiatica 23:135–151.

Szalay, F. S. 1984. Arboreality: is it homologous in metatherian and eutherian mammals? Evolutionary Biology 18:215–258.

——. 1994. Evolutionary history of the marsupials and an analysis of osteological characters. Cambridge University Press, New York.

Szalay, F. S., and E. J. Sargis. 2001. Model-based analysis of postcranial osteology of marsupials from the Palaeocene of Itaboraí (Brazil) and the phylogenetics and biogeography of Metatheria. Geodiversitas 23:139–302.

Tucker, V. A. 1970. Energetic cost of locomotion in animals. Comparative Biochemistry and Physiology 34:841–846.

——. 1975. The energetic cost of moving about. American Scientist 63:413–419.

Ungar, P. S., and M. Williamson. 2000. Exploring the effects of tooth wear on functional morphology: a preliminary study using dental topographic analysis. Palaeontologia Electronica 3:1–18.

Van Valen, L., and R. E. Sloan. 1977. Ecology and the extinction of the dinosaurs. Evolutionary Theory 2:37–64.

Van Valkenburgh, B. 1987. Skeletal indicators of locomotor behavior in living and extinct carnivores. Journal of Vertebrate Paleontology 7:162–182.

Van Valkenburgh, B., and K. P. Koepfli. 1993. Cranial and dental adaptations to predation in canids. Symposium of the Zoological Society of London 65:15–37.

Vázquez-Molinero, R., T. Martin, M. S. Fischer, and R. Frey. 2001. Comparative anatomical investigations of the postcranial skeleton of *Henkelotherium guimarotae* Krebs, 1991 (Eupantotheria, Mammalia) and their implications for its locomotion. Zoosystematics and Evolution 77:207–216.

Venables, W. N., and B. D. Ripley. 2002. Modern applied statistics with S. Springer, New York.

Weisbecker, V., and S. Schmid. 2007. Autopodial skeletal diversity in hystricognath rodents: functional and phylogenetic aspects. Mammalian Biology – Zeitschrift für Säugetierkunde 72:27–44.

Weisbecker, V., and D. I. Warton. 2006. Evidence at hand: diversity, functional implications, and locomotor prediction in intrinsic hand proportions of diprotodontian marsupials. Journal of Morphology 267:1469–1485.

Wilson, G. P. 2013. Mammals across the K/Pg boundary in northeastern Montana, U.S.A.: dental morphology and body-size patterns reveal extinction selectivity and immigrant-fueled ecospace filling. Paleobiology 39:429–469.

Wilson, D. E., and D. M. Reeder. 2005. Mammal species of the world: a taxonomic and geographic reference. Johns Hopkins University Press, Baltimore.

Wilson, G. P., A. R. Evans, I. J. Corfe, P. D. Smits, M. Fortelius, and J. Jernvall. 2012. Adaptive radiation of multituberculate mammals before the extinction of dinosaurs. Nature 483: 457–460.

Wing, S. L., and B. H. Tiffney. 1987. Interactions of angiosperms and herbivorous tetrapods through time. Pp. 203–224 *In* E. M. Friis, W. G. Chaloner, and P. R. Crane, eds. The origins of angiosperms and their biological consequences. Cambridge University Press, New York.

Yuan, C.-X., Q. Ji, Q.-J. Meng, A. R. Tabrum, and Z.-X. Luo. 2013. A new Jurassic mammal and origins of diverse feeding and locomotor adaptation multituberculate mammals. Science 341:779–783.

Zheng, X.-T., S.-D. Bi, X.-L. Wang, and J. Meng. 2013. A new arboreal haramiyid shows the diversity of crown mammals in the Jurassic period. Nature 500:199–202.

Zhou, C.-F., S.-Y. Wu, T. Martin, and Z.-X. Luo. 2013. A Jurassic mammaliaform and the earliest mammalian evolutionary adaptations. Nature 500:163–167.